



## Aminopyridinecarboxamide-based inhaled IKK-2 inhibitors for asthma and COPD: Structure–activity relationship

Jin Xie<sup>a,\*</sup>, Gennadiy I. Poda<sup>a</sup>, Yiding Hu<sup>c</sup>, Natalie X. Chen<sup>a</sup>, Richard F. Heier<sup>a</sup>, Serge G. Wolfson<sup>a</sup>, Matthew T. Reding<sup>a</sup>, Patrick J. Lennon<sup>a</sup>, Ravi G. Kurumbail<sup>a</sup>, Shaun R. Selness<sup>a</sup>, Xiong Li<sup>b</sup>, Nandini N. Kishore<sup>b</sup>, Cynthia D. Sommers<sup>b</sup>, Lori Christine<sup>b</sup>, Sheri L. Bonar<sup>b</sup>, Neetu Venkatraman<sup>b</sup>, Sumathy Mathialagan<sup>b</sup>, Sarah J. Brustkern<sup>b</sup>, Horng-Chih Huang<sup>a,\*</sup>

<sup>a</sup> Department of Medicinal Chemistry, Pfizer Inc., 700 Chesterfield Parkway West, St. Louis, MO 63017, United States

<sup>b</sup> Department of Biology, Pfizer Inc., 700 Chesterfield Parkway West, St. Louis, MO 63017, United States

<sup>c</sup> Department of Pharmacokinetics, Dynamics and Metabolism, Pfizer Inc., 700 Chesterfield Parkway West, St. Louis, MO 63017, United States

### ARTICLE INFO

#### Article history:

Received 13 October 2010

Revised 7 December 2010

Accepted 13 December 2010

Available online 23 December 2010

#### Keywords:

Potent  
Selective  
IKK-2  
Inhibitors  
Inhaled approach  
Asthma  
COPD  
DOA

### ABSTRACT

Installation of sites for metabolism in the lead compound **PHA-767408** was the key focus of the IKK-2 inhaled program. This paper reports our efforts to identify a novel series of aminopyridinecarboxamide-based IKK-2 inhibitors, which display low nanomolar potency against IKK-2 with long duration of action (DOA), and metabolically labile to phase I and/or phase II metabolizing enzymes with potential capability for multiple routes of clearance. Several compounds have demonstrated their potential usefulness in the treatment of asthma and chronic obstructive pulmonary disease (COPD).

© 2010 Elsevier Ltd. All rights reserved.

### 1. Introduction

Chronic obstructive pulmonary disease (COPD) is the 4th cause of death in the U.S. according to the '2007 NHLBI Morbidity and Mortality Chart Book'. An estimated 24 million US adults have COPD and 23 million have asthma. Protein kinases are believed to play a crucial role in the expression and activation of inflammatory mediators in the airways of patients with asthma and COPD.<sup>1</sup> Nuclear factor kappa  $\beta$  (NF- $\kappa$ B) is an inducible transcriptional activator that is activated in airway epithelium in asthma/COPD patients.<sup>2</sup> Normally, NF- $\kappa$ B is sequestered in the cytoplasm in an inactive form by the inhibitory I $\kappa$ B proteins. However, activation by oxidative stress (e.g., cigarette smoking) leads to activation of signaling cascades on the I $\kappa$ B kinase (IKK) complex, induces pulmonary inflammation, which results in a progressive decline in lung function.<sup>3</sup> Inhibition of NF- $\kappa$ B activity might, therefore, be an effective alternative approach to treat asthma and COPD. The

\* Corresponding authors. Tel.: +1 636 247 6251; fax: +1 636 247 5204 (J.X.).

E-mail addresses: [jin.xie@pfizer.com](mailto:jin.xie@pfizer.com) (J. Xie), [hhhuan01@hotmail.com](mailto:hhhuan01@hotmail.com) (H.-C. Huang).

core components of I $\kappa$ B kinase (IKK) complex include I $\kappa$ B kinase  $\alpha$  (IKK $\alpha$ , also known as IKK-1), I $\kappa$ B kinase  $\beta$  (IKK $\beta$ , also known as IKK-2) and NF- $\kappa$ B essential modulator (NEMO). IKK-2, the pivotal enzyme in the classical pathway of NF- $\kappa$ B activation, which is required for the expression of a range of inflammatory mediators associated with chronic lung inflammation characteristic of asthma and COPD, is therefore, an attractive target for pharmaceutical industry.<sup>4</sup> IKK-2 inhibitors have the potential to deliver a profound anti-inflammatory impact in a range of diseases.

Because of the key role played by the inhibition of IKK-2 in the activation of NF- $\kappa$ B, coupled with the druggability of protein kinases as a target class, a number of pharmaceutical companies have been pursuing drug discovery programs aimed at identifying IKK-2 inhibitors. These include thiophenecarboxamides,<sup>5</sup> indolecarboxamides,<sup>6</sup> substituted pyrazole ureas,<sup>7</sup> benzamides,<sup>8</sup> 2,4-diarylpyridines,<sup>9</sup> aminopyrimidines,<sup>10</sup>  $\beta$ -carbolines,<sup>11</sup> and pyrrolopyridines<sup>12</sup> and imidazo(1,2-a)thieno(3,2-e)pyrazines<sup>13</sup> derivatives. Bonafoux and Huang recently reported that the 8-(5-chloro-2-(4-methylpiperazin-1-yl)isonicotinamido)-1-(4-fluorophenyl)-4,5-dihydro-1H-benzo[g]indazole-3-carboxamide (**PHA-767408** or **PHA-408**), a selective, ATP-competitive inhibitor, which

binds IKK-2 tightly with a relatively slow off rate was efficacious in a chronic model of arthritis with no adverse effects at maximally efficacious doses.<sup>14</sup>

Figure 1 lists three scaffolds that were the focus of drug discovery efforts over the past several years in our labs. While the fully elaborated PHA-408 tricyclic pyrazole series show good selectivity for IKK-2 over other kinases, the smaller ureido-carboxamide scaffolds (PF-267 and PHA-495) are not as selective.<sup>5d,7</sup> The amide functionality, chloropyridyl group and the terminal piperazinyl group all contribute significantly to the overall potency of the PHA-408 series.<sup>14</sup> The core skeleton of PHA-408 exhibits low nM potency against IKK-2, excellent selectivity against a large panel of kinases, and encouragingly demonstrates a long duration of action (DOA).<sup>14c</sup> Many compounds in this series, however, have shown unfavorable pharmacokinetic characteristics, such as poor oral absorption, high clearance and low systemic exposure in pre-clinical species, and moderate margin over hERG inhibition.

Even though the optimization of this scaffold for an oral drug represents a lot of hurdles, including high protein binding and hERG activity for PHA-408, many of the properties of this scaffold lend themselves suitable for an inhaled drug to treat inflammatory lung disease, such as COPD and asthma. The IKK-2 inhibitor, as an anti-inflammatory agent, will be directly delivered to lung via inhalation, and take action on the pulmonary target. On the other hand, once the drug passes through lung into systemic circulation, it will be quickly cleared by hepatic metabolism to minimize the systemic exposure and subsequent cardiovascular event. The high clearance, mediated by hepatic metabolizing enzymes, is favorable in inhaled drug design. Thus, the metabolically unstable compounds are chosen from in vitro assay, for example, human liver microsomal (HLM) stability assay, as a drug candidate in lead selection and advancement. Ideal inhalation agents possess optimized pharmacodynamic properties, including target selectivity, potency and duration of action, and optimized pharmacokinetic properties, including high pulmonary deposition, prolonged pulmonary residence time, high systemic clearance and lower oral bioavailability to achieve high efficacy and minimized adverse effects related to the systemic exposure.<sup>15</sup> Thus we have chosen PHA-408 as a starting point for pulmonary drug delivery to achieve low nano-molecular potency, pharmacokinetic properties and safety.

This paper reports our efforts to identify drug candidates that are potent against IKK-2 enzyme, metabolically labile in human liver microsomes (HLM stability <30%<sup>14c</sup>), no/reduced hERG activity, long duration of action, and demonstrating the capacity for multiple routes of clearance to minimize systemic exposure and manage potential drug–drug interaction (DDI) risks.

## 2. Chemistry

We launched a medicinal chemistry program to explore the SAR around the PHA-408 lead to improve potency, cellular activity,

DOA and favorable pharmacokinetic properties required for an inhaled drug, while maintaining the core structure and key binding elements of PHA-408 for excellent selectivity. We have explored modifications on the Southern domain independently by incorporating functional groups to the terminal piperazinyl to enhance metabolic liability mediated by the phase I metabolizing enzymes, mainly cytochromes P450 in the liver. We have also optimized the Northern domain, with an aim of incorporation of metabolic ‘handles’ for rapid clearance, in particular, phenols for phase II conjugation. Combination of the phase I and phase II metabolic pathways, that is, multiple clearance mechanisms, are expected to reduce the risk of potential drug–drug interactions observed with a single clearance route (Fig. 2). A variety of combinations in the Northern domain and the Southern domain led us to investigate several chemical series.

### 2.1. Southern domain modification: divergent synthetic efforts

Most of the N-substituted pyrazolyl-aminopyridine-3-carboxamides **1** were obtained, with yields ranging from 40% to 85%, by reacting the previously reported PHA-801 with commercially available pyrazole aldehydes through reductive amination using sodium triacetoxyborohydride or resin-bound cyanoborohydride (Scheme 1).

Compound **2a** was synthesized by reductive amination of PHA-801 with ethyl 2-(4-formyl-1H-pyrazol-1-yl) acetate using sodium triacetoxyborohydride. Subsequent amidation of **2a** with various amines in methanol (Scheme 2) led predominantly to the desired product **3**. It is worth noting that it required long reaction times and higher temperature for secondary amines and also resulted in lower yields of products leading to troublesome purifications and modest yields.

Compound **4** was synthesized by reductive amination of PHA-801 with 2-(4-formyl-1H-pyrazol-1-yl) acetic acid using sodium triacetoxyborohydride. Subsequent esterification of **4** with various alcohols in the presence of thionyl chloride (Scheme 3) gave the desired products **5** in yields ranging from 60% to 80%.

Compound **6** was synthesized by reductive amination of PHA-801 with 1H-pyrazole-4-carbaldehyde using sodium triacetoxyborohydride. Subsequent alkylation of **6** with various alkyl bromides in the presence of sodium hydride in DMF gave the desired products **7** in yields ranging from 60% to 80% (Scheme 4).

### 2.2. Northern domain modification

Synthetic Scheme 5 illustrates a six step procedure used for the preparation of analogs **13**, **14**, **15**, **16**, **17**, **18**, **19** and **20**. Nitrotetralone was converted into the diketo ester enolate **8** following the literature.<sup>14d</sup> The diketo ester enolate **8** was refluxed with corresponding R1- and/or R2- substituted phenylhydrazine in acetic acid to give pyrazole intermediate **9**. For **16**, **17**, **18**, **19**, substituted

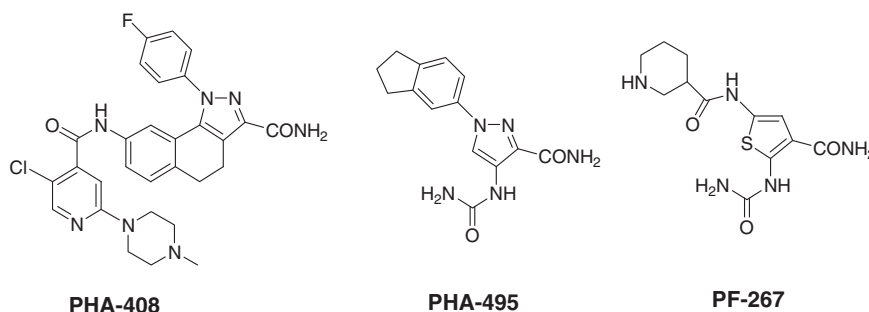
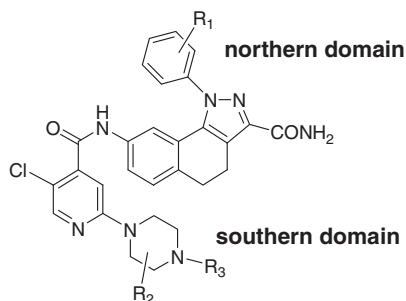


Figure 1. IKK-2 inhibitors series developed by Pfizer.

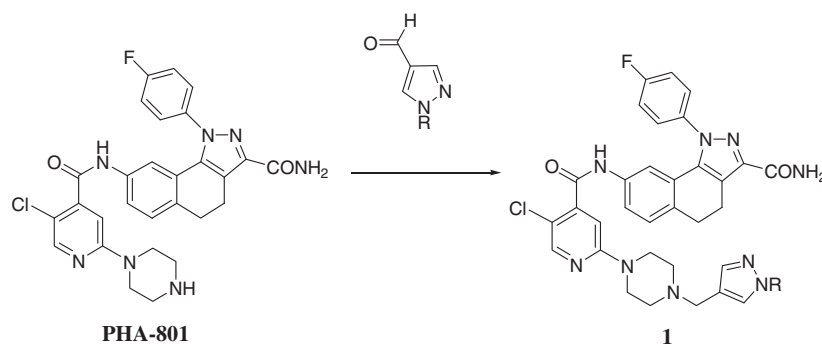


**Figure 2.** Strategy for exploring the SAR around PHA-408.

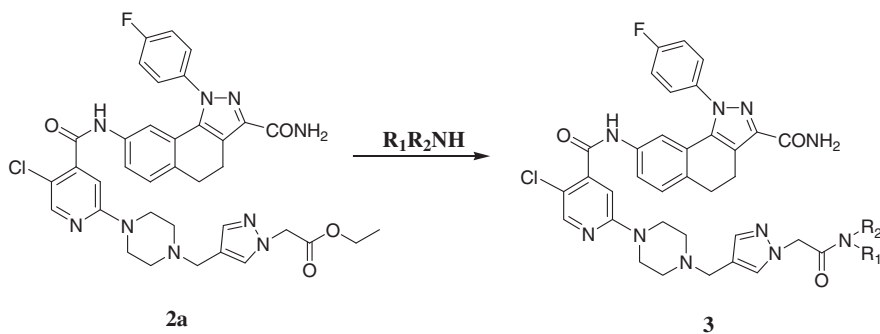
methoxyphenyl hydrazines were used to give the corresponding pyrazoles **9**. Then the nitro group was reduced to amine by using

zinc dust in ethanol to give corresponding intermediates **10**. In the following step, the conversion of ester to amide was achieved by reacting with liquid ammonia in a pressured tube at high temperature to give amides **11**. The resulting amides **11** can react with 2,5-dichloroisonicotinic acid in pyridine to give the desired intermediates **12**. Direct amination of intermediates **12** with *N*-methylpiperazine afforded the desired products **13**, **14**, **15** and **20** with satisfactory yields. For **16**, **17**, **18**, **19**, demethylation of intermediate **12** was carried out first in the presence of boron tribromide, then the crude intermediates were mixed with *N*-methylpiperazine and refluxed overnight to give the corresponding final products **16**, **17**, **18**, **19** with moderate yields.

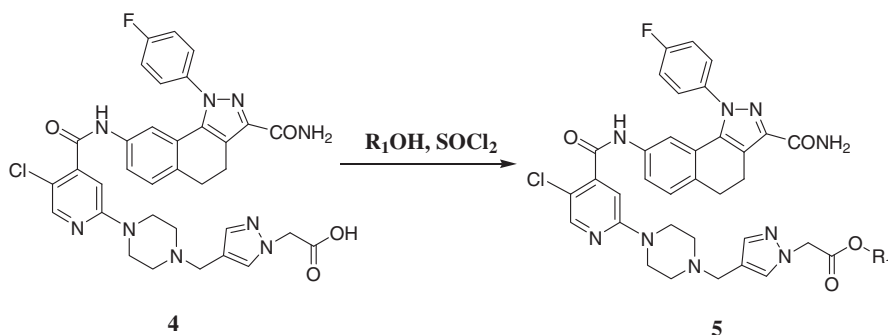
1-(3-Chloro-4-methoxyphenyl)hydrazine **21** (Scheme 6) was synthesized by treatment of 3-chloro-4-methoxyaniline in concentrated hydrochloric acid at 0 °C with a solution of sodium nitrite in water, then reduced by stannous chloride to give final product **21** (31% yield).



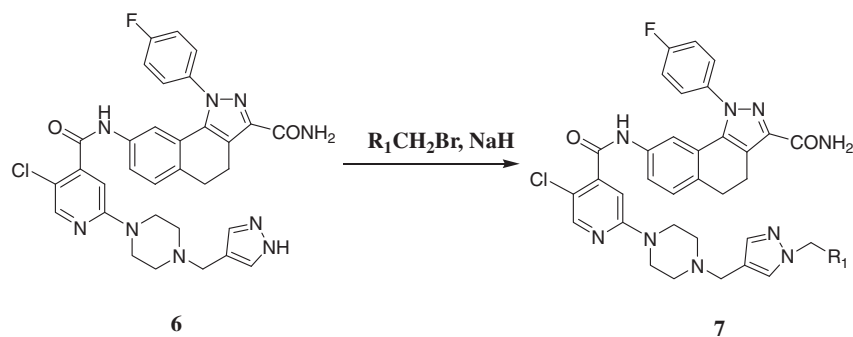
**Scheme 1.** Reagents and conditions: pyrazole aldehyde (1.5 equiv), sodium triacetoxyborohydride (2.5 equiv), DMSO, rt.



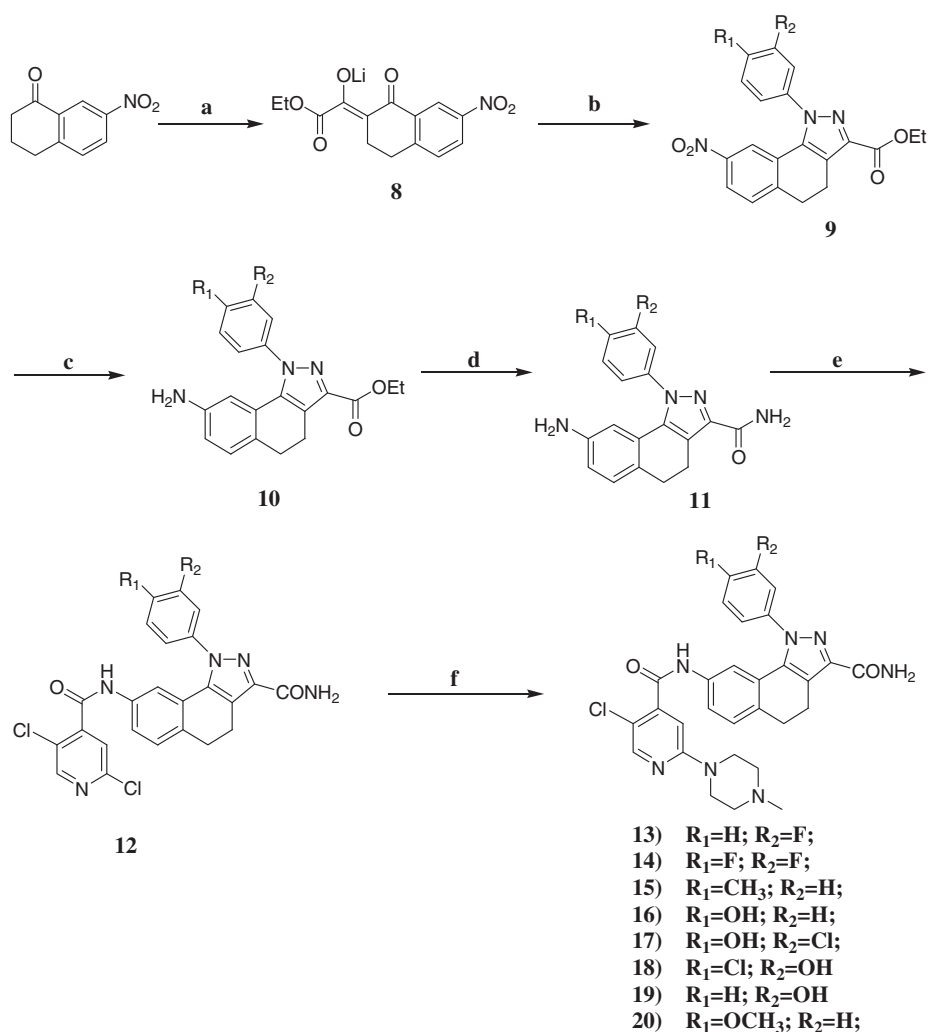
**Scheme 2.** Reagents:  $R_1R_2NH$  (10 equiv),  $CH_3OH$ .



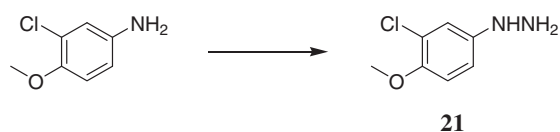
**Scheme 3.** Reagents and conditions: (a) ROH (excess),  $SOCl_2$ , 80 °C.



**Scheme 4.** Reagents and conditions: (a)  $R_1CH_2Br$  (1.2 equiv), NaH (1.5 equiv), rt.



**Scheme 5.** Reagents and conditions: (a) ethyl oxalate (1.2 equiv), lithium bis(trimethylsilyl) amide in ether, rt; (b) substituted phenylhydrazine hydrochloride (1.2 equiv), acetic acid, 80 °C, 16 h; (c) zinc dust (excess), acetic acid, ethanol; (d) ethanolic ammonia (1:1); (e) 2,5-dichloroisonicotinic acid (1.2 equiv), HBTU, diisopropylethyl amine, DMF; (f) boron tribromide (10 equiv) 16 h; then *N*-methylpiperazine, reflux.



**Scheme 6.** Reagents: (a) sodium nitrite, then stannous chloride in concentrated HCl.

### 3. Biology

The synthesized inhibitors were initially evaluated for inhibition of recombinant human IKK-2.<sup>16,17</sup> Compounds with an  $IC_{50}$  on IKK-2 less than 5 nM were subsequently tested in the human peripheral blood mononuclear cells (PBMC) screen.<sup>14c</sup> The PBMC assay was our primary cell-based assay, used to measure inhibitory effects of IKK-2 inhibitors on the functional response of lipopolysaccharide (LPS)

stimulated TNF- $\alpha$  release from PBMC. The results of this assay were used to determine if a compound has reasonable cell permeation in vitro, therefore, advanced further for in vitro and in vivo testing. Compounds with an IC<sub>50</sub> on human PBMC less than 50 nM subsequently progressed for the DOA studies in enzymatic and cell-based assays to determine the dissociation rate constants for human IKK-2 and human PBMC cells.<sup>14c</sup>

#### 4. Molecular modeling

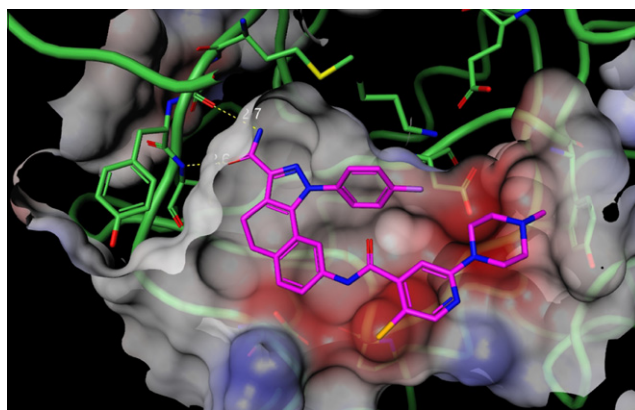
IKK-2 is a large protein kinase molecule (756 amino acids) with several structural modules including an N-terminal protein kinase domain, a leucine-zipper motif and a coiled-coiled domain.<sup>18</sup> To our knowledge, there is no known crystal structure of IKK-2 reported in the literature. However, we have generated homology models of IKK-2 based on crystal structures of cAMP-dependent protein kinase (PKA)<sup>19</sup> and CHK-1 kinase.<sup>20</sup> The homology model of IKK-2 was built using a PKA *in house* crystal structure as a template in the complex with a fused pyrrolopyrimidine analog that was not structurally similar to **PHA-408**. However, the kinase domain of this high resolution protein structure was fully resolved (without any unresolved residues neither in the Gly-rich loop nor in the activation loop) and the Phe residue (Phe54 in PKA) at the very tip of the Gly-rich loop was pointing towards the solvent allowing more room for the initial placement of the ligands for the IFD docking. The O14920 sequence of the human IKK-2 was retrieved from SwissProt and used to build the homology model. We performed a BLAST search using the first 300 amino acids that correspond to the kinase domain of IKK-2. Three proteins were identified with highest sequence identity: death-associated protein kinase 1 (DAPK1, 32% sequence identity), p21-activated kinase 1 (PAK1, 30% sequence identity) and PKA (30% sequence identity). All three kinases (DAPK1, PAK1 and PKA) have 7 amino acids in the hinge region as IKK-2 does. This fact does not speak in favor of any of these templates. PKA has an advantage over DAPK1 since it has the same gate-keeper residue (Met, M96 in IKK-2) as IKK-2 does while DAPK1 has Leu (L93). While PAK1 also has Met (M344) as gate-keeper, it has Arg residue (R299) instead of the solvent-exposed Lys across the hinge (K106 in IKK-2). As a result of the homology modeling procedure, the Cartesian coordinates for the structurally-conserved regions have been assigned from PKA and the loops that had insertions in the sequence alignment were built, sampled and energy minimized afterwards while keeping the rest of the protein fixed and the tethering positional constraints were gradually released. The ATP binding site of IKK-2 was pre-shaped by placing **PHA-408** optimized at Becke3LYP/6-31G\* level with Jaguar (version 6.5, 2005, Schrödinger, LLC, New York, NY) from its putative IKK-2-bound conformation, and the whole protein-ligand complex was refined via the multi-step energy minimization procedure with first the ligand and the protein backbone fixed, followed by gradually released tethering positional constraints on the protein backbone and the ligand (ff91, 4r dielectric constant, RMS gradients <0.1 kcal/mol Å<sup>2</sup>). The conformation of the A-loop in the IKK-2 homology model is the weakest part. However, with the exception of Tyr169, the residue followed the conserved DFG motif (DLG in IKK-2) in protein kinases, no other residues were in close contact with **PHA-408**.

We used the Induced Fit Docking (IFD) procedure from Schrödinger<sup>21</sup> to dock **PHA-408** and its analogs. First, the protein and ligand van der Waals radii have been scaled down to 0.5 and 20 docking poses were generated using standard precision (SP) Glide scoring. Second, a 6 Å shell of residues around the Ligand was minimized with Prime. Finally, the ligands were docked with extra precision (XP) scoring followed up with post-docking minimization for each of 20 poses.

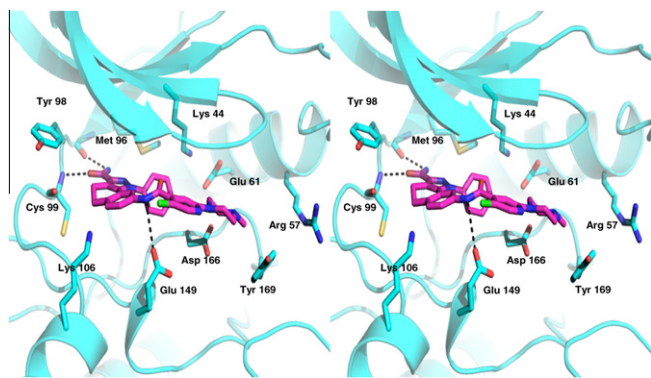
#### 5. Results and discussion

Figure 3a and b below show **PHA-408** docked into the IKK-2 homology model following the IFD procedure described above. When docking new synthetic targets and rationalizing SAR some ligands were observed to flip 180° allowing the carboxamide portion of **PHA-408** to bind to both the backbone NH and carbonyl of Cys99 or the backbone NH of Cys99 and backbone carbonyl of Gln97. The identified docked orientation consistent with major SAR but does not explain all modifications, and we do not have any direct experimental evidence regarding the possible binding mode. Based on the docking experiments, we believe that the carboxamide moiety of the inhibitor forms interactions with the hinge region of the IKK-2 ATP binding site (Fig. 3a and b). 4-Fluorophenyl binds deep in the pocket towards the methionine gate-keeper Met96. The molecule occupies the adenine, sugar and phosphate sub-sites of ATP with the piperazine moiety nearby the conserved catalytic Asp166, the  $\alpha$ C-helix and the activation loop. Substituents of the piperazine ring would be binding right outside of the ATP site phosphate region towards the activation loop and would be either partially solvent-exposed or engaging the A-loop via weak solvent-exposed interactions. With **PHA-408** demonstrating some DOA and based on its binding mode we thought that placing groups of the piperazine ring towards the A-loop,  $\alpha$ C-helix or solvent front would either preserve or improve this effect in most cases. This strategy has been proven successful.

As previously disclosed,<sup>14</sup> **PHA-408** was potent in IKK-2 enzyme and cellular assays and further demonstrated promising duration of action. As a pulmonary delivered drug candidate for treatment of COPD, its in vitro pharmacologic profile requires good DOA in enzyme and cell-based assays, high clearance in liver microsomal stability assays, rapid in vivo clearance and poor systemic exposure. Multiple routes of elimination are preferred to mitigate potential clinical DDI. To identify new candidates with better DOA in enzyme and cell-based assays, a small SAR set of analogs was designed and synthesized to explore the Northern portion of the molecule. As shown in Table 1, most modifications to the phenyl group resulted in potent IKK-2 inhibitors in both enzyme and cellular assays. In addition, UDP-glucuronosyltransferases (UGT) catalyzed phase II metabolism was involved in the clearance of this scaffold of compounds when a hydroxy group was introduced. Particularly, acidic chlorophenol demonstrated rapid glucuronidation clearance in vitro, when substitution groups are properly arranged, such as analog **17** (data not shown). However, the loss of DOA in the



**Figure 3a.** Top view of **PHA-408** docked into IKK-2 homology model following the Induced Fit Docking procedure from Schrödinger, Inc. The Gly-rich loop is hidden for clarity and the ATP IKK-2 binding site depicted by the Connolly surface color-coded by the calculated Electrostatic Potential (red color for negative electrostatic potential and blue color for positive electrostatic potential).



**Figure 3b.** Side-by-side stereo view of **PHA-408** docked in IKK-2. H-bonds between the protein and the ligand are shown by bold dotted lines. Only key residues in proximity to the ligand are shown for clarity.

enzymatic assay was observed with the chlorophenolic analogs, **17** and **18**. Based on the proposed binding mode in the IKK-2 homology model, bulky substitution on the phenyl ring could lead to unfavorable clashes with the protein and the Southern moiety, which could adopt an alternative conformation with the piperazine ring turning toward the kinase solvent front, resulting in the loss of DOA. With that hypothesis in mind, we then redirected our attention to modifications of the Southern region.

The second set of analogs was designed to probe SAR around piperazine and their effect on DOA, while maintaining or enhancing the metabolic liability. A few of those compounds were exemplified in Table 2. Replacement of the methylpiperazine ring in **PHA-408** with a hydroxypiperidine or a linear methoxyethylamine, resulted in analogs (**PF-296** and **PF-544**, respectively) with great potency in enzyme and cellular assays, but again with no DOA in the enzymatic assay. A methoxyethyl group on the piperazine yielded **PHA-919**, a very potent IKK-2 inhibitor in the cells, however, it also lost the DOA. Pyrazoyl methyl substitution on the piperazine has led to a potent compound **22a** and with good DOA. A focused library was thus constructed to fine-tune the SAR around the pyrazoyl moiety.

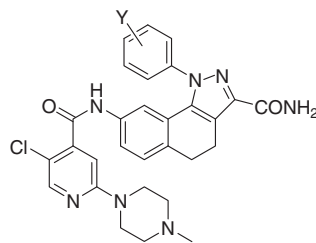
In Table 3 were shown pairs of compounds with variations in both the pyrazole and the phenyl rings to demonstrate translatability of the DOA effect from simultaneous variations. Similar to the simple methyl piperazines shown in Table 1 (**PHA-408** and **13**), 3- and 4-fluoro analogs (**22b** and **22a**) were equipotent in enzyme and cells with similar enzyme DOA, albeit slightly shorter  $t_{1/2}$  for the 3-fluorophenyl analog. Replacing the methyl with an ethoxyacetyl group led to a pair of compounds with great potency and DOA in both enzyme and cells. These compounds showed short half life in HLM, were highly metabolized by microsomal enzymes, including cytochromes P450s and possibly esterases. However, binding in the competition dofetilide (DOF) assay (a radiolabeled ligand to the hERG or  $K_v11.1$  potassium ion channel) was also high, indicating the increased risk of potential adverse cardiovascular side effects.

Before expanding the SAR around the pyrazoyl nitrogen, we also took time to explore the effect of substitutions on the piperazine and pyrazole rings. As shown in Table 4, methyl substitution on either rings in the piperazinyl pyrazole, (**41**, **42**, and **43**) resulted in analogs of similar enzyme potency as the parent lead compound **22a**. Even though the enzyme DOA was all >4 h, translation from the enzyme into cell potency varies. Unsubstituted pyrazoles (**22a** and **43**) showed only 2–3-folds right shift, while **41** and **42** (enzyme DOA = 8 h) showed much bigger cell-to-enzyme ratio (20–30-folds). For the two carboxylic acid analogs off the piperazine ring (**44** and **45**), the analog with distal carboxyl group from pyrazole was more potent in enzymatic assay and had better enzyme DOA. However, the enzyme-to-cell translation was understandably much worse for both analogs with >100-fold right shift due to their poor permeability. At the moment, we do not have reasonable explanations for the observed right shift in the enzyme-to-cell activity translation. Most potent inhibitors have poor permeability, which might lead to great right shift from enzyme to cell potency.

Summarizing the results from these brief SAR studies, we concluded that the quickest route to minimize the DOF inhibitory effect and optimize DOA and cell potency was to focus on derivatization of N-substitutions on the pyrazole ring.

In Table 5, comparing **22a** with the unsubstituted analog **6**, the methyl group does not seem to affect the in vitro properties, such

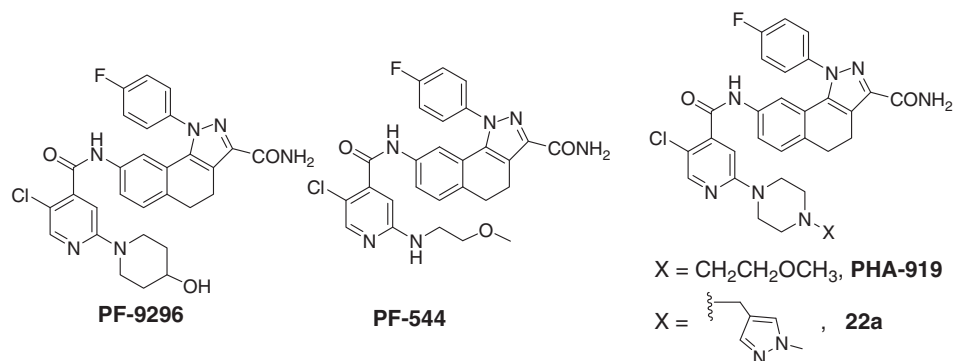
**Table 1**  
Effect of substituent on the Northern phenyl group on inhibition of IKK-2\*



CPD	Y=	IKK-2 IC <sub>50</sub> (nM)	PBMC IC <sub>50</sub> (nM)	Enzyme $t_{1/2}$ (h)
PHA-408	4-Fluoro	1.6	39	3
<b>13</b>	3-Fluoro	4.8	14	2
<b>14</b>	3,4-Difluoro	10	65	
<b>15</b>	4-Methyl	14	38	0
<b>16</b>	4-Hydroxy	3.5	75	1
<b>17</b>	3-Chloro-4-hydroxy	2.8	46	1
<b>18</b>	3-Hydroxy-4-chloro	2.2		1
<b>19</b>	3-Hydroxy	1.2	89	1
<b>20</b>	4-Methoxy	6.1	33	0

\* Inhibition of kinase activity was assessed as described under *Materials and Methods*. IC<sub>50</sub> data are expressed as a mean of three or more experiments and standard deviations were within 50% of the reported value. Dissociation kinetics  $t_{1/2}$  from rhIKK-2 and PBMC cell activity were determined as described under *Materials and Methods*.

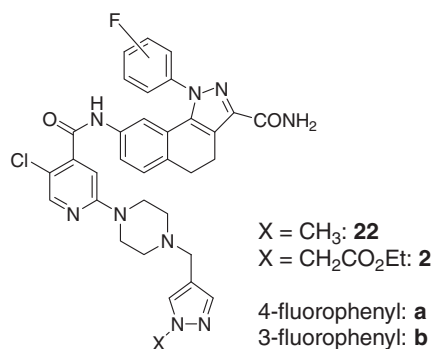
**Table 2**  
Effect of the Southern region substitutions on duration of action in enzymatic assay\*



CPD	hIKK-2 IC <sub>50</sub> (nM)	PBMC IC <sub>50</sub> (nM)	Enzyme t <sub>1/2</sub> (h)
PHA-408	1.6	39	2.8
PF-296	0.6	15	0.1
PF-544	0.6	134	0.1
PHA-919	1.9	8	0.6
<b>22a</b>	3	11	4

\* Inhibition of kinase activity was assessed as described under *Materials and Methods*. IC<sub>50</sub> data are expressed as a mean of three or more experiments and standard deviations were within 50% of the reported value. Dissociation kinetics t<sub>1/2</sub> from rhIKK-2 and PBMC cell activity were determined as described under *Materials and Methods*.

**Table 3**  
Analogues with variation in both Northern and Southern regions\*



CPD	IKK-2 IC <sub>50</sub> (nM)	PBMC IC <sub>50</sub> (nM)	Enzyme t <sub>1/2</sub> (h)	Cell t <sub>1/2</sub> (h)	HLM t <sub>1/2</sub> (min)	DOF (% of effect)
<b>22a</b>	3	11	4		17	91
<b>22b</b>	2	14	3		14	83
<b>2a</b>	1	6	5	>4	3	95
<b>2b</b>	5	9	5	>4	3	78

\* Inhibition of kinase activity was assessed as described under *Materials and Methods*. IC<sub>50</sub> data are expressed as a mean of three or more experiments and standard deviations were within 50% of the reported value. Dissociation kinetics for both enzyme and cell t<sub>1/2</sub>, PBMC cell activity, human liver microsomal clearance, and DOF inhibition experiments were determined as described under *Materials and Methods*.

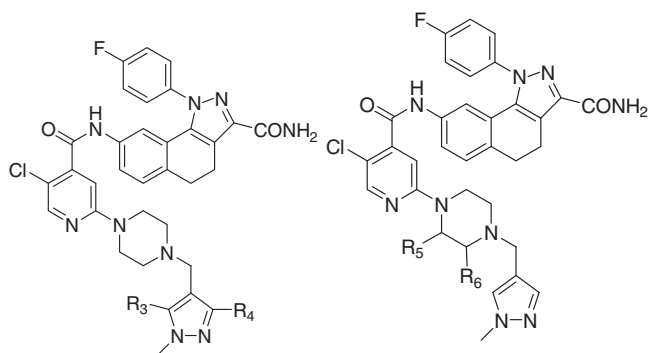
as potency, DOA, HLM stability and DOF inhibitory effect. The simple ethyl analog, **23**, has a better DOA, but its cellular potency has dropped significantly. Further functionalization of the ethyl group with cyano, ether, alcohol or amine, all leads to very potent inhibitors (**24**, **25**, **26**, **27** and **28**) in both enzyme and cells. With the exception of longer ether **26** which lost DOA in the cellular assay, these compounds all maintained the DOA in both enzyme and cells, and desirable high clearance in HLM, but also showed similar DOF liability which was alleviated slightly with more hydrophilic substituents such as alcohols or amines. Alkoxyacetyls (**29**, **2a**, **30** and **31**) showed very similar properties in all aspects as analogs just discussed. The corresponding carboxylic acid **4** is very potent in enzyme with a big right shift in the cell assay, and good DOA, but due to its higher hydrophilicity it showed low clearance and

DOF inhibition. This trend was also observed in the amide analogs, more hydrophilic analogs, such as primary amide **32** and secondary amide with a hydroxy tail **38**; tend to have low clearance and DOF inhibition and bigger right shift in the cellular assay. Surprisingly they also have shorter DOA in the cellular assay. The tertiary amide with bis-hydroxy tail **39** and a secondary amide with a longer amino tail **40** both showed low DOF inhibition.

## 6. Conclusion

In an effort to rationalize the SAR of DOA in the **PHA-408** series, and to minimize DOF inhibition effect while maintaining desirable high clearance, we explored two regions in the lead compound **PHA-408** which are amenable to structural modifications with

**Table 4**  
Effect of pyrazolyl substitution on duration of action in enzyme\*



**22a:** R<sub>3</sub> = H; R<sub>4</sub> = H  
**41:** R<sub>3</sub> = H; R<sub>4</sub> = CH<sub>3</sub>  
**42:** R<sub>3</sub> = CH<sub>3</sub>; R<sub>4</sub> = H  
**43:** X = CH<sub>3</sub>; R<sub>5</sub> = H; R<sub>6</sub> = CH<sub>3</sub>  
**44:** X = CH<sub>3</sub>; R<sub>5</sub> = CO<sub>2</sub>H; R<sub>6</sub> = H  
**45:** X = CH<sub>3</sub>; R<sub>5</sub> = H; R<sub>6</sub> = CO<sub>2</sub>H

CPD	IKK-2 IC <sub>50</sub> (nM)	PBMC IC <sub>50</sub> (nM)	Enzyme t <sub>1/2</sub> (h)
<b>22a</b>	3.2	11	4
<b>41</b>	4.3	118	8
<b>42</b>	2.8	67	8
<b>43</b>	3.5	9	6
<b>44</b>	0.5	529	4.2
<b>45</b>	3.9	432	0.3

\* Inhibition of kinase activity was assessed as described under *Materials and Methods*. IC<sub>50</sub> data are expressed as a mean of three or more experiments and standard deviations were within 50% of the reported value. Dissociation kinetics t<sub>1/2</sub> from rhIKK-2 and PBMC cell activity were determined as described under *Materials and Methods*.

little or no penalty on potency. The effort was guided by the IKK-2 homology model and docking experiments that allow partial protein flexibility at the binding site. Based on the proposed binding mode of **PHA-408** it was hypothesized that substituents of piperazine would either maintain or improve the duration of action in enzymatic and cell-based assays at least for best analogs. This hypothesis was proven to be successful. Indeed, it was found that a small heterocycle attached to the piperazine ring can be substituted with various hydrophilic tails to reduce DOF inhibition and still maintain cell potency and DOA. We have also demonstrated that slow offset from the IKK-2 enzyme translates into an extended DOA in *in vitro* washout assays. In summary, **27**, **28** and **40** have the best overall properties in potency, DOA, HLM, DOF and no hERG activity. The three compounds were advanced for further characterization in the expanded kinase selectivity panel, *in vivo* pharmacokinetic profiling and *in vivo* inhaled COPD efficacy models. The results from these studies will be reported in due time.

## 7. Experimental section

### 7.1. General methods and materials

Column chromatography was performed using 200–400 mesh silica gels. <sup>1</sup>H NMR and <sup>13</sup>C NMR were obtained on Varian Inova-300 and Varian Inova-400 spectrometers using DMSO-*d*<sub>6</sub> as the internal standard. For some compounds, peaks near the water signal are missing, and exchangeable protons may also be missing due to water in the sample. Mass spectra (MS) were recorded with a Micromass ZMD spectrometer. High resolution mass spectra were recorded using a Perceptive Biosystems Mariner TOF mass spectrometer. Elemental analysis was performed by Atlantic MicroLab, GA.

### 7.2. IKK-2 enzyme assay (rhIKK-2)

The detailed IKK-2 Enzyme assay was described previously.<sup>15,16</sup> In brief, electroplated 96-well plates were coated with anti-phospho-IκBα (Santa Cruz Biochemicals, Santa Cruz, CA) at a concentration of 5 pmol/well. All kinase assays were performed in a 30-μl total volume for 90 min in kinase buffer containing 25 mM HEPES, 10 mM NaF, 0.1% bovine serum, albumin, 0.0005% Triton X-100, 5 mM MnCl<sub>2</sub>, 5 mM MgCl<sub>2</sub>, 1 mM dithiothreitol, and 2% Me<sub>2</sub>SO, pH 7.5. For rhIKK-2 activity, inhibitor and rhIKK-2 (0.1 nmol/well) were added simultaneously to plates with substrate (1 μM ATP, 2 μM biotinylated IκBα Ser32-Ala36 peptide). The reaction was stopped by washing the plates twice with Tris-buffered saline/Tween 20. Electrochemiluminescence was generated by adding sulfo-tagged streptavidin (25 μl/well) for 1 h and following the manufacturer's (MesoScale Discovery) instructions. Phospho-IκBα levels were quantified with the use of a Sector Imager 6000 (MesoScale Discovery). Specific IKK kinase was determined by subtracting values from a non-peptide control.

### 7.3. IKK-2 PBMC cellular assay

Primary cell culture has been described previously.<sup>15</sup> In brief; human whole blood was collected from healthy donors in sodium-heparinized tubes (BD, Franklin Lakes, NJ). Neutrophils or PBMC were isolated by Ficoll separation. Cells were resuspended in RPMI 1640 medium with penicillin-streptomycin (10 U/ml) and 5% FBS and plated into 96-well culture plates at 2.5 × 10<sup>5</sup> cells/well. Compounds were added to the cells and incubated for 1 h before a 16-h LPS (20 ng/ml) stimulation. Supernatants were collected and placed in new 96-well plate for analysis for TNFα release by ELISA.

### 7.4. Human IKK-2 t<sub>1/2</sub> off-rate determination

The dissociation rate constants of compounds from human IKK-2 were determined by following the recovery of the human IKK-2 kinase activity under the following conditions. Compounds were pre-incubated (25–100 nM) with 25 nM of human IKK-2 for 1 h at room temperature. The kinase reaction was started with the addition of 100 mM ATP and 1 mM 5-fluorescein (FAM)-GRHDSGLDSMK-NH<sub>2</sub>. The kinase activity was followed over time using a Caliper Lab Chip 3000. All reactions were carried out in 25 mM Hepes, 5 mM MgCl<sub>2</sub>, 5 mM MnCl<sub>2</sub>, 10 mM NaF, 0.1% BSA, and 1 mM DTT at pH 7.5. All data were best fit using Grafit 4.0.

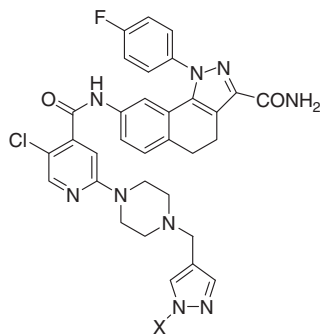
### 7.5. IKK-2 PBMC cell DOA

Using frozen cell technology, the PBMCs were thawed and plated into 96-well plates. Compounds were added to the cells and incubated for 1 h. Then after 1 h the compounds were washed off four times, by spinning the 96-well plate and removing all the supernatant. The control plate was not washed. Then the plates were either stimulated for 4 h with LPS, or some time was allowed to pass for DOA purposes (0.5 h or 24 h) before stimulation. The supernatant was then assayed for TNFα release via MSD technology.

### 7.6. Human liver microsomal stability

Analog (1 μM) were incubated in human liver microsomes (0.8 mg/ml) with the addition of a NADPH-regenerating system (1 mM NADP<sup>+</sup>, 5 mM isocitric acid, 1 unit/ml isocitric acid dehydrogenase) in 100 mM potassium phosphate buffer (pH 7.4) for 30 min. Acetonitrile with internal standard was added to stop

**Table 5**  
Effect of pyrazole substituents on in vitro properties\*



CPD	X=	hIKK2 IC <sub>50</sub> (nM)	PBMC IC <sub>50</sub> (nM)	Enzyme t <sub>1/2</sub> (h)	Cell t <sub>1/2</sub> (h)	HLM t <sub>1/2</sub> (min)	DOF (% of effect)
<b>6</b>	H	1.9	16	3		8	78
<b>22a</b>	Methyl	3.2	11	4		17	91
<b>23</b>	Ethyl	4.2	102	>8			
<b>24</b>	CH <sub>2</sub> CH <sub>2</sub> CN	7.6	9	5	>4	6	98
<b>25</b>	(CH <sub>2</sub> ) <sub>3</sub> OCH <sub>3</sub>	2.8	16	4	>4	3	76
<b>26</b>	(CH <sub>2</sub> ) <sub>3</sub> OCH <sub>2</sub> CH <sub>2</sub> OCH <sub>3</sub>	6.6	21	4	<4	3	69
<b>27</b>	(CH <sub>2</sub> ) <sub>3</sub> OH	2.2	15	5	>4	9	49
<b>28</b>	(CH <sub>2</sub> ) <sub>3</sub> N(CH <sub>3</sub> ) <sub>2</sub>	3.7	12	4	>4	11	42
<b>29</b>	CH <sub>2</sub> CO <sub>2</sub> CH <sub>3</sub>	1.1	54	6			24
<b>2a</b>	CH <sub>2</sub> CO <sub>2</sub> CH <sub>2</sub> CH <sub>3</sub>	1.3	6	5	>4	3	95
<b>30</b>	CH <sub>2</sub> CO <sub>2</sub> CH <sub>2</sub> CH <sub>2</sub> OCH <sub>3</sub>	1.3	9	4	>4	3	66
<b>31</b>	CH <sub>2</sub> CH <sub>2</sub> CO <sub>2</sub> CH <sub>2</sub> CH <sub>3</sub>	4.7	14	6	>4	3	90
<b>4</b>	CH <sub>2</sub> CO <sub>2</sub> H	0.5	221	5	4	120	29
<b>32</b>	CH <sub>2</sub> CONH <sub>2</sub>	0.9	7	5	<4	58	38
<b>33</b>	CH <sub>2</sub> CONHCH <sub>3</sub>	1.4	15	6	>4	13	57
<b>34</b>	CH <sub>2</sub> CONH( <i>i</i> -propyl)	2.0	36	5			94
<b>35</b>	CH <sub>2</sub> CON(CH <sub>3</sub> ) <sub>2</sub>	2.3	13	5	<4	8	50
<b>36</b>	CH <sub>2</sub> CONH(CH <sub>2</sub> ) <sub>2</sub> OCH <sub>3</sub>	1.3	10	6	>4	3	58
<b>37</b>	CH <sub>2</sub> CONH(CH <sub>2</sub> ) <sub>2</sub> SCH <sub>3</sub>	2.5	10	4	4	3	98
<b>38</b>	CH <sub>2</sub> CONH(CH <sub>2</sub> ) <sub>2</sub> OH	1.0	9	5	<4	120	12
<b>39</b>	CH <sub>2</sub> CON((CH <sub>2</sub> ) <sub>2</sub> OH) <sub>2</sub>	10.2	474	4	>4		-1
<b>40</b>	CH <sub>2</sub> CONH(CH <sub>2</sub> ) <sub>3</sub> N(CH <sub>3</sub> ) <sub>2</sub>	3.3	26	6		36	34

\* Inhibition of kinase activity was assessed as described under *Materials and Methods*. IC<sub>50</sub> data are expressed as a mean of three or more experiments and standard deviations were within 50% of the reported value. Dissociation kinetics t<sub>1/2</sub> for both enzyme and cell, PBMC cell activity, human liver microsomal clearance, and DOF inhibition experiments were determined as described under *Materials and Methods*.

the reaction. The reaction mixture was centrifuged, and supernatant was analyzed for test compound by liquid chromatography coupled to tandem mass spectrometry, and t<sub>1/2</sub> (min) was reported.

### 7.7. Dofetilide binding

The dofetilide competitive binding assay is performed using a 384-well fluorescence polarization method. The assay is conducted using HEK-293 cell membranes transfected with the hERG protein. The compounds of interest are allowed to compete for binding to the potassium channel (I<sub>Kr</sub>) along with Cy3B tagged *N*-desmethyl dofetilide. Assay plates are read using a Tecan Safire2.

### 7.8. General procedure for reductive amination using sodium triacetoxyborohydride for compound 1

Sodium triacetoxyborohydride (2.5 equiv) was added to a solution of PF-2687138 (1 equiv) and an appropriate aldehyde (1.5 equiv) in 0.5 mL DMSO with acetic acid (2 equiv) and stirred at room temperature for 2 h. The reaction was filtered through a 0.45 μm PTFE membrane syringe filter and evaporated overnight using a nitrogen stream. The material was purified using reverse-phase chromatography with acetonitrile/water as the mobile phase.

### 7.9. General procedure for reductive amination using resin-bound cyanoborohydride for compound 1

Silica-bound cyanoborohydride resin (1.5 equiv) was added to a solution of PF-2687138 (1 equiv) and an appropriate aldehyde (1.5 equiv) in 1 mL of DMSO/acetic acid (70/30) and agitated on an orbit shaker for 18 h. The reaction was filtered through a 0.45 μm PTFE membrane syringe filter and was purified using reverse-phase chromatography with acetonitrile/water as the mobile phase.

### 7.10. General procedure for amidation for compound 3

Mixture of 0.065 mM of compound **2a** and 10 equiv of primary amines in 3 ml MeOH was stirred at rt overnight. After the solvent was removed, the residue was re-dissolved in 1 ml DMSO and purified using reverse-phase chromatography with acetonitrile/water as the mobile phase.

### 7.11. General procedure for esterification for compound 5

Mixture of 0.058 mM of compound **4** in 1 mL alcohol was added 2 equiv SOCl<sub>2</sub>, the mixture was heated to 80 °C and stirred overnight. After the solvent was removed, the residue was re-dissolved in 1 ml DMSO and purified using reverse-phase chromatography with acetonitrile/water as the mobile phase.

## 7.12. General procedure for N-alkylation for compound 7

To a slurry of sodium hydride (1.5 equiv) in 1 mL DMF at 0 °C was added compound **6** (1 equiv). The mixture was stirred for 30 min; an appropriate alkyl bromide (1.2 equiv) of 0.058 mM of compound **4** was added. The reaction mixture was warmed up to rt, and stirred overnight. After the solvent was removed, the residue was re-dissolved in 1 ml DMSO and purified using reverse-phase chromatography with acetonitrile/water as the mobile phase.

### 7.12.18-((5-Chloro-2-[4-(1H-pyrazol-4-ylmethyl)piperazin-1-yl]isonicotinoyl)amino)-1-(4-fluorophenyl)-4,5-dihydro-1H-benzo[g]indazole-3-carboxamide (**6**)

Prepared using the general reductive amination procedure. <sup>1</sup>H NMR (DMSO-*d*<sub>6</sub>, 400 MHz): δ ppm 2.12–2.57 (m, 8H) 2.70–3.07 (m, 4H) 3.34–3.62 (m, 2H) 6.82 (s, 1H) 7.10–7.68 (m, 12H) 8.10 (s, 1H) 10.25 (s, 1H); HRMS (M+H) calcd for C<sub>32</sub>H<sub>30</sub>ClFN<sub>9</sub>O<sub>2</sub> 626.2117, found 626.2037.

### 7.12.2. 8-[(5-Chloro-2-[4-[(1-methyl-1H-pyrazol-4-yl)methyl]piperazin-1-yl]isonicotinoyl)amino]-1-(4-fluorophenyl)-4,5-dihydro-1H-benzo[g]indazole-3-carboxamide (**22a**)

Prepared using the general reductive amination procedure. <sup>1</sup>H NMR (DMSO-*d*<sub>6</sub>, 400 MHz): δ ppm 2.22–2.50 (m, 8H) 2.81–2.95 (m, 4H) 3.40–3.49 (m, 2H) 3.74 (s, 3H) 6.84 (s, 1H) 7.19 (d, *J* = 1.83 Hz, 1H) 7.23–7.42 (m, 6H) 7.49–7.60 (m, 4H) 8.10 (s, 1H) 10.30 (s, 1H); HRMS (M+H) calcd for C<sub>33</sub>H<sub>32</sub>ClFN<sub>9</sub>O<sub>2</sub> 640.2273, found 640.2233.

### 7.12.3. 8-[(5-Chloro-2-[4-[(1-methyl-1H-pyrazol-4-yl)methyl]piperazin-1-yl]isonicotinoyl)amino]-1-(4-fluorophenyl)-4,5-dihydro-1H-benzo[g]indazole-3-carboxamide (**4**)

Prepared using the general reductive amination procedure. <sup>1</sup>H NMR (400 MHz, DMSO-*d*<sub>6</sub>) δ ppm 2.25–2.50 (m, 8H) 2.81–2.95 (m, 4H) 3.40–3.49 (m, 2H) 4.86 (s, 2H) 6.86 (s, 1H) 7.19–7.26 (m, 1H) 7.28–7.42 (m, 6H) 7.49–7.60 (m, 4H) 8.13 (s, 1H) 10.28 (s, 1H); HRMS (M+H) calcd for C<sub>34</sub>H<sub>32</sub>ClFN<sub>9</sub>O<sub>4</sub> 684.2172, found 684.2154.

### 7.12.4. 8-[[2-(4-[[1-(2-Amino-2-oxoethyl)-1H-pyrazol-4-yl]methyl]piperazin-1-yl)-5-chloroisonicotinoyl]amino]-1-(4-fluorophenyl)-4,5-dihydro-1H-benzo[g]indazole-3-carboxamide (**32**)

Prepared using the general reductive amination procedure. <sup>1</sup>H NMR (DMSO-*d*<sub>6</sub>, 400 MHz): δ ppm 2.55–2.68 (m, 4H) 2.94–3.09 (m, 6H) 3.47 (s, 2H) 3.53–3.64 (m, 4H) 4.78 (s, 2H) 6.96 (s, 1H) 7.28–7.36 (m, 1H) 7.40–7.52 (m, 5H) 7.56–7.62 (m, 1H) 7.62–7.72 (m, 3H) 7.93–8.02 (m, 1H) 8.22 (s, 1H) 10.38 (s, 1H); HRMS (M+H) calcd for C<sub>34</sub>H<sub>33</sub>ClFN<sub>10</sub>O<sub>3</sub> 683.2331, found 683.2361.

### 7.12.5. 8-[(5-Chloro-2-[4-[(1-[2-(dimethylamino)-2-oxoethyl]-1H-pyrazol-4-yl)methyl]piperazin-1-yl]isonicotinoyl)amino]-1-(4-fluorophenyl)-4,5-dihydro-1H-benzo[g]indazole-3-carboxamide (**35**)

<sup>1</sup>H NMR (400 MHz, DMSO-*d*<sub>6</sub>) δ ppm 2.36–2.46 (m, 4H) 2.82 (s, 3H) 2.85–2.97 (m, 4H) 2.99 (s, 3H) 3.35–3.55 (m, 6H) 5.01 (s, 2H) 6.87 (s, 1H) 7.19–7.64 (m, 10H) 8.13 (s, 1H) 10.29 (s, 1H); LRMS (M+H) calcd for C<sub>36</sub>H<sub>37</sub>ClFN<sub>10</sub>O<sub>3</sub> 711.2, found 711.2.

### 7.12.6. 8-[(5-Chloro-2-[4-[(1-[2-(isopropylamino)-2-oxoethyl]-1H-pyrazol-4-yl)methyl]piperazin-1-yl]isonicotinoyl)amino]-1-(4-fluorophenyl)-4,5-dihydro-1H-benzo[g]indazole-3-carboxamide (**34**)

<sup>1</sup>H NMR (DMSO-*d*<sub>6</sub>, 400 MHz): δ ppm 1.04 (d, *J* = 6.59 Hz, 6H) 2.33–2.44 (m, 4H) 2.85–2.92 (m, 4H) 3.37 (s, 2H) 3.43–3.53 (m, 4H) 3.72–3.88 (m, 1H) 4.26–4.34 (m, 1H) 4.65 (s, 2H) 6.86 (s,

1H) 7.22 (m, 3H) 7.33–7.55 (m, 8H) 8.07–8.15 (m, 1H) 10.27 (s, 1H); LRMS (M+H) calcd for C<sub>37</sub>H<sub>39</sub>ClFN<sub>10</sub>O<sub>3</sub> 725.3, found 725.3.

### 7.12.7. 8-[(5-Chloro-2-[4-[(1-[2-(methylamino)-2-oxoethyl]-1H-pyrazol-4-yl)methyl]piperazin-1-yl]isonicotinoyl)amino]-1-(4-fluorophenyl)-4,5-dihydro-1H-benzo[g]indazole-3-carboxamide (**33**)

<sup>1</sup>H NMR (DMSO-*d*<sub>6</sub>, 400 MHz): δ ppm 2.56–2.60 (m, 1H) 2.68 (d, *J* = 4.39 Hz, 3H) 2.95–3.09 (m, 6H) 3.47 (s, 3H) 3.53–3.64 (m, 5H) 4.78 (s, 2H) 6.96 (s, 1H) 7.28–7.36 (m, 2H) 7.40–7.52 (m, 4H) 7.59 (s, 1H) 7.62–7.72 (m, 3H) 7.93–8.02 (m, 1H) 8.22 (s, 1H) 10.38 (s, 1H); LRMS (M+H) calcd for C<sub>35</sub>H<sub>35</sub>ClFN<sub>10</sub>O<sub>3</sub> 697.3, found 697.3.

### 7.12.8. 8-[[5-Chloro-2-(4-[[1-(2-[[3-(dimethylamino)propyl]amino]-2-oxoethyl]-1H-pyrazol-4-yl]methyl]piperazin-1-yl]isonicotinoyl)amino]-1-(4-fluorophenyl)-4,5-dihydro-1H-benzo[g]indazole-3-carboxamide (**40**)

<sup>1</sup>H NMR (DMSO-*d*<sub>6</sub>, 400 MHz): δ ppm 1.53 (t, *J* = 6.95 Hz, 2H) 2.11 (s, 6H) 2.22 (t, *J* = 6.77 Hz, 2H) 2.38–2.48 (m, 4H) 2.94 (d, *J* = 9.52 Hz, 4H) 3.10 (q, *J* = 6.59 Hz, 2H) 3.39 (s, 3H) 3.45–3.56 (m, 5H) 4.71 (s, 2H) 6.88 (s, 1H) 7.21–7.28 (m, 2H) 7.32–7.44 (m, 4H) 7.52 (s, 1H) 7.56–7.63 (m, 2H) 7.93–8.01 (m, 1H) 8.15 (s, 1H) 10.30 (s, 1H); LRMS (M+H) calcd for C<sub>39</sub>H<sub>44</sub>ClFN<sub>11</sub>O<sub>3</sub> 768.3, found 768.3.

### 7.12.9. 8-[[5-Chloro-2-[4-[(1-[2-[(2-hydroxyethyl)amino]-2-oxoethyl]-1H-pyrazol-4-yl)methyl]piperazin-1-yl]isonicotinoyl]amino]-1-(4-fluorophenyl)-4,5-dihydro-1H-benzo[g]indazole-3-carboxamide (**38**)

<sup>1</sup>H NMR (DMSO-*d*<sub>6</sub>, 400 MHz): δ ppm 2.34–2.45 (m, 4H) 2.93 (d, *J* = 9.15 Hz, 4H) 3.15 (q, *J* = 5.98 Hz, 2H) 3.36–3.47 (m, 5H) 3.47–3.57 (m, 4H) 4.63–4.70 (m, 1H) 4.73 (s, 2H) 6.88 (s, 1H) 7.20–7.28 (m, 2H) 7.32–7.44 (m, 4H) 7.47–7.54 (m, 1H) 7.54–7.64 (m, 2H) 7.92–8.02 (m, 1H) 8.14 (s, 1H) 10.30 (s, 1H); LRMS (M+H) calcd for C<sub>36</sub>H<sub>37</sub>ClFN<sub>10</sub>O<sub>4</sub> 727.2, found 727.3.

### 7.12.10. 8-[[2-(4-[[1-(2-[[Bis(2-hydroxyethyl)amino]-2-oxoethyl]-1H-pyrazol-4-yl)methyl]piperazin-1-yl]-5-chloroisonicotinoyl)amino]-1-(4-fluorophenyl)-4,5-dihydro-1H-benzo[g]indazole-3-carboxamide (**39**)

<sup>1</sup>H NMR (DMSO-*d*<sub>6</sub>, 400 MHz): δ ppm 2.42 (s, 4H) 2.93 (d, *J* = 9.15 Hz, 4H) 3.15 (q, *J* = 5.98 Hz, 2H) 3.36–3.47 (m, 7H) 3.47–3.57 (m, 6H) 4.63–4.70 (m, 1H) 5.08 (s, 2H) 6.88 (s, 1H) 7.20–7.28 (m, 2H) 7.32–7.44 (m, 4H) 7.47–7.54 (m, 1H) 7.54–7.64 (m, 2H) 7.92–8.02 (m, 1H) 8.14 (s, 1H) 10.30 (s, 1H); LRMS (M+H) calcd for C<sub>38</sub>H<sub>41</sub>ClFN<sub>10</sub>O<sub>5</sub> 771.3, found 771.3.

### 7.12.11. 8-[(5-Chloro-2-[4-[(1-[2-[(2-methoxyethyl)amino]-2-oxoethyl]-1H-pyrazol-4-yl)methyl]piperazin-1-yl]isonicotinoyl)amino]-1-(4-fluorophenyl)-4,5-dihydro-1H-benzo[g]indazole-3-carboxamide (**36**)

<sup>1</sup>H NMR (DMSO-*d*<sub>6</sub>, 400 MHz): δ ppm 2.34–2.44 (m, 4H) 2.85–2.99 (m, 4H) 3.38 (br s, 3H) 3.45–3.55 (m, 5H) 4.72 (s, 2H) 6.86 (s, 1H) 7.22 (br s, 2H) 7.27–7.65 (m, 8H) 7.98–8.07 (m, 1H) 8.12 (s, 1H) 10.28 (s, 1H); LRMS (M+H) calcd for C<sub>37</sub>H<sub>39</sub>ClFN<sub>10</sub>O<sub>4</sub> 741.3, found 741.3.

### 7.12.12. 8-[[5-Chloro-2-(4-[[1-(2-[[2-(methylthio)ethyl]amino]-2-oxoethyl]-1H-pyrazol-4-yl]methyl]piperazin-1-yl]isonicotinoyl)amino]-1-(4-fluorophenyl)-4,5-dihydro-1H-benzo[g]indazole-3-carboxamide (**37**)

<sup>1</sup>H NMR (DMSO-*d*<sub>6</sub>, 400 MHz): δ ppm 2.05 (s, 2H) 2.38–2.48 (m, 5H) 2.88–3.00 (m, 5H) 3.40 (s, 3H) 3.51 (s, 6H) 4.74 (s, 2H) 6.88 (s, 1H) 7.22–7.28 (m, 2H) 7.32–7.44 (m, 4H) 7.51–7.54 (m, 1H) 7.56–

7.64 (m, 3H) 8.07–8.18 (m, 2H) 10.30 (s, 1H); LRMS (M+H) calcd for  $C_{37}H_{39}ClFN_{10}O_3S$  757.2, found 757.3.

**7.12.13. Methyl [4-({4-[4-({[3-(aminocarbonyl)-1-(4-fluorophenyl)-4,5-dihydro-1H-benzo[g]indazol-8-yl]amino}carbonyl)-5-chloropyridin-2-yl]piperazin-1-yl)methyl]-1H-pyrazol-1-yl] acetate (29)**

$^1H$  NMR (DMSO- $d_6$ , 400 MHz):  $\delta$  ppm 2.25–2.50 (m, 4H) 2.81–2.95 (m, 4H) 3.39 (s, 3H) 3.43–3.53 (m, 6H) 4.86 (s, 2H) 6.86 (s, 1H) 7.19–7.26 (m, 2H) 7.28–7.66 (m, 9H) 8.13 (s, 1H) 10.28 (s, 1H); LRMS (M+H) calcd for  $C_{35}H_{34}ClFN_9O_4$  698.2, found 698.3.

**7.12.14. Ethyl [4-({4-[4-({[3-(aminocarbonyl)-1-(4-fluorophenyl)-4,5-dihydro-1H-benzo[g]indazol-8-yl]amino}carbonyl)-5-chloropyridin-2-yl]piperazin-1-yl)methyl]-1H-pyrazol-1-yl] acetate (2a)**

$^1H$  NMR (DMSO- $d_6$ , 400 MHz):  $\delta$  ppm 1.19 (t,  $J = 7.14$  Hz, 2H) 2.41 (s, 4H) 2.88–3.00 (m, 4H) 3.40 (s, 3H) 3.45–3.57 (m, 5H) 4.13 (q,  $J = 6.95$  Hz, 2H) 5.00 (s, 2H) 6.88 (s, 1H) 7.25 (d, 2H) 7.32–7.44 (m, 4H) 7.51 (s, 1H) 7.59 (dd,  $J = 8.42, 4.76$  Hz, 2H) 7.63 (s, 1H) 8.15 (s, 1H) 10.31 (s, 1H); LRMS (M+H) calcd for  $C_{36}H_{36}ClFN_9O_4$  712.3, found 712.3.

**7.12.15. Ethyl 3-[4-({4-[4-({[3-(aminocarbonyl)-1-(4-fluorophenyl)-4,5-dihydro-1H-benzo[g]indazol-8-yl]amino}carbonyl)-5-chloropyridin-2-yl]piperazin-1-yl)methyl]-1H-pyrazol-1-yl] propanoate (31)**

$^1H$  NMR (DMSO- $d_6$ , 400 MHz):  $\delta$  ppm 1.12 (t,  $J = 7.05$  Hz, 3H) 2.31–2.43 (m, 4H) 2.80 (t,  $J = 6.50$  Hz, 2H) 2.84–3.01 (m, 4H) 3.34 (s, 2H) 3.41–3.54 (m, 4H) 3.95–4.08 (m, 2H) 4.28 (t,  $J = 6.59$  Hz, 2H) 6.85 (s, 1H) 7.19–7.26 (m, 1H) 7.27–7.43 (m, 7H) 7.48 (s, 1H) 7.52–7.61 (m, 2H) 8.12 (s, 1H) 10.28 (s, 1H); LRMS (M+H) calcd for  $C_{37}H_{38}ClFN_9O_4$  726.3, found 726.3.

**7.12.16. 8-({5-Chloro-2-[4-({1-[3-(dimethylamino)propyl]-1H-pyrazol-4-yl)methyl]piperazin-1-yl]isonicotinoyl}amino)-1-(4-fluorophenyl)-4,5-dihydro-1H-benzo[g]indazole-3-carboxamide (28)**

$^1H$  NMR (DMSO- $d_6$ , 400 MHz):  $\delta$  ppm 1.82 (t,  $J = 6.85$  Hz, 2H) 2.02–2.13 (m, 8H) 2.36 (t,  $J = 4.70$  Hz, 4H) 2.83–2.97 (m, 4H) 3.34 (s, 2H) 3.41–3.51 (m, 4H) 4.03 (t,  $J = 6.98$  Hz, 2H) 6.86 (s, 1H) 7.20 (d,  $J = 2.15$  Hz, 1H) 7.25–7.44 (m, 6H) 7.49–7.62 (m, 4H) 8.12 (s, 1H) 10.31 (s, 1H); LRMS (M+H) calcd for  $C_{37}H_{41}ClFN_{10}O_2$  711.3, found 711.3.

**7.12.17. 8-({5-Chloro-2-[4-({1-(2-cyanoethyl)-1H-pyrazol-4-yl)methyl]piperazin-1-yl]isonicotinoyl}amino)-1-(4-fluorophenyl)-4,5-dihydro-1H-benzo[g]indazole-3-carboxamide (24)**

$^1H$  NMR (DMSO- $d_6$ , 400 MHz):  $\delta$  ppm 2.38 (t,  $J = 4.56$  Hz, 4H) 2.86–2.96 (m, 4H) 3.00 (t,  $J = 6.31$  Hz, 2H) 3.36 (s, 2H) 3.41–3.51 (m, 4H) 4.31 (t,  $J = 6.31$  Hz, 2H) 6.87 (s, 1H) 7.21 (d,  $J = 1.88$  Hz, 1H) 7.25–7.45 (m, 6H) 7.49–7.61 (m, 3H) 7.68 (s, 1H) 8.12 (s, 1H) 10.31 (s, 1H); LRMS (M+H) calcd for  $C_{35}H_{33}ClFN_{10}O_2$  679.2, found 679.2.

**7.12.18. 8-({5-Chloro-2-[4-({1-(3-hydroxypropyl)-1H-pyrazol-4-yl)methyl]piperazin-1-yl]isonicotinoyl}amino)-1-(4-fluorophenyl)-4,5-dihydro-1H-benzo[g]indazole-3-carboxamide (27)**

Prepared using the general reductive amination general procedure.  $^1H$  NMR (DMSO- $d_6$ , 400 MHz):  $\delta$  ppm 2.83–2.97 (m, 4H) 3.30–3.36 (m, 4H) 3.42–3.54 (m, 4H) 4.07 (t,  $J = 6.98$  Hz, 2H) 4.52 (t,  $J = 5.10$  Hz, 1H) 6.86 (s, 1H) 7.21 (d,  $J = 1.88$  Hz, 1H) 7.25–7.43 (m, 6H) 7.50–7.62 (m, 4H) 8.12 (s, 1H) 10.31 (s, 1H); LRMS (M+H) calcd for  $C_{35}H_{36}ClFN_9O_3$  684.2, found 684.2.

**7.12.19. 8-({5-Chloro-2-[4-({1-(3-methoxypropyl)-1H-pyrazol-4-yl)methyl]piperazin-1-yl]isonicotinoyl}amino)-1-(4-fluorophenyl)-4,5-dihydro-1H-benzo[g]indazole-3-carboxamide (25)**

$^1H$  NMR (DMSO- $d_6$ , 400 MHz):  $\delta$  ppm 1.93 (t,  $J = 6.58$  Hz, 2H) 2.36 (t,  $J = 4.56$  Hz, 4H) 2.80–2.97 (m, 4H) 3.18 (s, 3H) 3.22 (t,  $J = 6.18$  Hz, 2H) 3.34 (s, 2H) 3.46 (d,  $J = 4.83$  Hz, 4H) 4.06 (t,  $J = 6.98$  Hz, 2H) 6.86 (s, 1H) 7.20 (d,  $J = 1.88$  Hz, 1H) 7.24–7.43 (m, 6H) 7.50–7.60 (m, 4H) 8.12 (s, 1H) 10.31 (s, 1H); HRMS (M+H) calcd for  $C_{36}H_{38}ClFN_9O_3$  698.2692, found 698.2799.

**7.12.20. 8-({5-Chloro-2-[4-({1-[3-(2-methoxyethoxy)propyl]-1H-pyrazol-4-yl)methyl]piperazin-1-yl]isonicotinoyl}amino)-1-(4-fluorophenyl)-4,5-dihydro-1H-benzo[g]indazole-3-carboxamide (26)**

$^1H$  NMR (DMSO- $d_6$  and water, 400 MHz):  $\delta$  ppm 1.88–2.04 (m, 2H) 2.34–2.46 (m, 4H) 2.84–3.06 (m, 4H) 3.25 (s, 1H) 3.31–3.36 (m, 3H) 3.36–3.59 (m, 11H) 4.10 (t,  $J = 6.77$  Hz, 2H) 6.87 (s, 1H) 7.19–7.60 (m, 11H) 8.14 (s, 1H) 10.30 (s, 1H); LRMS (M+H) calcd for  $C_{38}H_{42}ClFN_9O_4$  742.3, found 742.3.

**7.12.21. 8-({5-Chloro-2-[4-({1-(methyl-1H-pyrazol-4-yl)methyl]piperazin-1-yl]isonicotinoyl}amino)-1-(3-fluorophenyl)-4,5-dihydro-1H-benzo[g]indazole-3-carboxamide (22b)**

Prepared using the general reductive amination general procedure.  $^1H$  NMR (DMSO- $d_6$ , 400 MHz):  $\delta$  ppm 2.30–2.42 (m, 8H) 2.83–3.01 (m, 4H) 3.39–3.55 (m, 2H) 3.79 (s, 3H) 6.87 (s, 1H) 7.20–7.67 (m, 12H) 8.12 (s, 1H) 10.31 (s, 1H); LRMS (M+H) calcd for  $C_{33}H_{32}ClFN_9O_2$  640.3, found 640.3.

**7.12.22. Ethyl [4-({4-[4-({[3-(aminocarbonyl)-1-(3-fluorophenyl)-4,5-dihydro-1H-benzo[g]indazol-8-yl]amino}carbonyl)-5-chloropyridin-2-yl]piperazin-1-yl)methyl]-1H-pyrazol-1-yl] acetate (2b)**

Prepared using the general reductive amination general procedure.  $^1H$  NMR (DMSO- $d_6$ , 400 MHz):  $\delta$  ppm 1.19 (t,  $J = 7.14$  Hz, 2H) 2.41 (s, 4H) 2.88–3.00 (m, 4H) 3.40 (s, 3H) 3.45–3.57 (m, 5H) 4.13 (q,  $J = 6.95$  Hz, 2H) 5.00 (s, 2H) 6.88 (s, 1H) 7.20–7.67 (m, 12H) 8.12 (s, 1H) 10.31 (s, 1H); LRMS (M+H) calcd for  $C_{36}H_{36}ClFN_9O_4$  712.3, found 712.3.

**7.12.23. 8-({5-Chloro-2-[4-methylpiperazin-1-yl]isonicotinoyl}amino)-1-(3-fluorophenyl)-4,5-dihydro-1H-benzo[g]indazole-3-carboxamide (13)**

$^1H$  NMR (DMSO- $d_6$ , 400 MHz):  $\delta$  ppm 2.32 (s, 3H) 2.40–2.45 (m, 4H) 2.92–3.09 (m, 4H) 3.52–3.67 (m, 4H) 6.97 (s, 1H) 7.27–7.72 (m, 9H) 8.22 (s, 1H) 10.39 (s, 1H); LRMS (M+H) calcd for  $C_{29}H_{28}ClFN_7O_2$  560.2, found 560.2.

**7.12.24. 8-({5-Chloro-2-((3S)-3-methyl-4-({1-(methyl-1H-pyrazol-4-yl)methyl]piperazin-1-yl]isonicotinoyl}amino)-1-(4-fluorophenyl)-4,5-dihydro-1H-benzo[g]indazole-3-carboxamide (43)**

$^1H$  NMR (DMSO- $d_6$ , 400 MHz):  $\delta$  ppm 1.10 (d, 3H,  $J = 6.3$  Hz), 2.05–2.35 (m, 2H), 2.65–2.79 (m, 2H), 2.87–2.93 (m, 6H), 3.60–3.74 (m, 1H), 3.76 (s, 3H) 3.90–4.0 (m, 2H), 6.85 (s, 1H), 7.21–7.65 (m, 11H), 8.11 (s, 1H), 10.31 (s, 1H); LRMS (M+H) calcd for  $C_{34}H_{34}ClFN_9O_2$  654.2, found 654.2.

**7.12.25. 4-({4-([3-Carbamoyl-1-(4-fluorophenyl)-4,5-dihydro-1H-benzo[g]indazol-8-yl]carbamoyl)-5-chloropyridin-2-yl]-[(1-methyl-1H-pyrazol-4-yl)methyl]piperazine-2-carboxylic acid (45)**

Prepared using the general reductive amination general procedure.  $^1H$  NMR (DMSO- $d_6$ , 400 MHz):  $\delta$  ppm 2.17 (m, 1H) 2.79–3.00 (m, 9H) 3.75 (s, 3H) 3.80–4.0 (m, 2H), 6.85 (s, 1H),

7.21–7.65 (m, 11H), 8.11 (s, 1H), 10.31 (s, 1H); LRMS (M+H) calcd for  $C_{34}H_{32}ClFN_9O_4$  684.2, found 684.2.

**7.12.26. 1-(4-[[3-Carbamoyl-1-(4-fluorophenyl)-4,5-dihydro-1H-benzo[g]indazol-8-yl]carbamoyl]-5-chloropyridin-2-yl)-4-[(1-methyl-1H-pyrazol-4-yl)methyl]piperazine-2-carboxylic acid (44)**

Prepared using the general reductive amination general procedure.  $^1H$  NMR (DMSO- $d_6$ , 400 MHz):  $\delta$  ppm 1.60–2.0 (m, 4H) 2.72–2.82 (m, 1H) 2.83–3.02 (m, 6H) 3.45–3.60 (m, 2H) 3.75 (s, 3H) 3.80–3.95 (s, 1H), 4.29–4.38 (s, 1H) 6.55 (s, 1H), 7.15–7.65 (m, 11H), 8.11 (s, 1H), 10.31 (s, 1H); LRMS (M+H) calcd for  $C_{34}H_{32}ClFN_9O_4$  684.2, found 684.2.

**7.12.27. 8-[[5-Chloro-2-(4-methylpiperazin-1-yl)isonicotinoyl]amino]-1-(3,4-difluorophenyl)-4,5-dihydro-1H-benzo[g]indazole-3-carboxamide (14)**

Prepared using the general reductive amination general procedure.  $^1H$  NMR (DMSO- $d_6$ , 400 MHz):  $\delta$  ppm 2.34 (s, 3H), 2.40–2.45 (m, 4H), 2.87–2.93 (m, 4H), 3.47 (m, 4H), 6.87 (s, 1H), 7.20–7.65 (m, 8H), 8.13 (s, 1H), 10.31 (s, 1H); LRMS (M+H) calcd for  $C_{29}H_{27}ClF_2N_7O_2$  578.2, found 578.2.

**7.12.28. Ethyl 1-(4-methoxyphenyl)-8-nitro-4,5-dihydro-1H-benzo[g]indazole-3-carboxylate (9: R1 = OCH<sub>3</sub>; R2 = H)**

To a solution of compound **8**<sup>14a</sup> (55 g, 0.19 mol) in 830 mL of 1:1 glacial acetic acid and absolute ethanol, 4-methoxyphenylhydrazine hydrochloride (35 g, 0.2 mol) was added and stirred at 80 °C for 16 h under nitrogen. The reaction mixture was then cooled to 0–5 °C and filtered. The residue was washed with cold ether and dried to afford compound **9** (64 g, 88%) as brownish yellow solid.  $^1H$  NMR (400 MHz, DMSO- $d_6$ ):  $\delta$  1.30–1.33 (m, 3H), 3.01–3.04 (m, 2H), 3.08–3.12 (m, 2H), 3.85 (s, 3H), 4.32 (q, 2H,  $J = 7.1$  Hz), 7.17 (d, 2H,  $J = 8.8$  Hz), 7.41 (d, 1H,  $J = 2.1$  Hz), 7.52 (d, 2H,  $J = 8.8$  Hz), 7.67 (d, 1H,  $J = 8.2$  Hz), 8.07 (dd, 1H,  $J = 2.2, 8.3$  Hz); LRMS (M+H) calcd for  $C_{21}H_{20}N_3O_5$  394.1, found 394.1.

**7.12.29. Ethyl 8-amino-1-(4-methoxyphenyl)-4,5-dihydro-1H-benzo[g]indazole-3-carboxylate (10: R1 = OCH<sub>3</sub>; R2 = H)**

Compound **9** (64 g, 0.16 mol) was dissolved in 1.28 L of acetic acid and 640 mL of ethanol. Zinc dust (85.38 g, 1.31 mol) was added in portions at 5–10 °C with stirring over a 30 min period. After addition of the zinc dust was completed, the reaction mixture was allowed to stir at 23 °C for 1 h. The completion of the reaction was monitored by thin layer chromatography. The reaction mixture was then filtered through a bed of Celite and washed with ethyl acetate (3 × 150 mL). The filtrate was diluted with dichloromethane (2.5 L) then neutralized (pH 7) with saturated sodium bicarbonate solution. The organic layer was separated and washed with water and brine successively, dried over anhydrous sodium sulfate and evaporated to dryness to afford 65 g of crude product. This material was recrystallized twice with 7:3 dichloromethane: hexane giving 31.5 g (53.3%) of compound **10** as a yellow solid.  $^1H$  NMR (400 MHz, DMSO- $d_6$ ):  $\delta$   $^1H$  NMR (400 MHz, DMSO- $d_6$ ):  $\delta$  1.30–1.33 (m, 3H), 3.01–3.04 (m, 2H), 3.08–3.12 (m, 2H), 3.85 (s, 3H), 4.32 (q, 2H,  $J = 7.1$  Hz), 7.17 (d, 2H,  $J = 8.8$  Hz), 7.41 (d, 1H,  $J = 2.1$  Hz), 7.52 (d, 2H,  $J = 8.8$  Hz), 7.67 (d, 1H,  $J = 8.2$  Hz), 8.07 (dd, 1H,  $J = 2.2, 8.3$  Hz); LRMS (M+H) calcd for  $C_{21}H_{22}N_3O_3$  364.1, found 364.1.

**7.12.30. 8-Amino-1-(4-methoxyphenyl)-4,5-dihydro-1H-benzo[g]indazole-3-carboxamide (11, R1 = OCH<sub>3</sub>; R2 = H)**

Compound **10** (15 g, 0.04 mol) was treated with 750 mL of ethanolic ammonia (1:1) solution at –78 °C inside a 2 l autoclave vessel. The reaction mixture was slowly warmed to 23 °C and then heated to 120 °C for 48 h. The reaction mixture was then cooled to 23 °C and was transferred to a round bottomed flask and

evaporated to dryness to obtain compound **11** (13.75 g, >95%) as a yellow solid.  $^1H$  NMR (400 MHz, DMSO- $d_6$ ):  $\delta$  2.72 (t, 2H,  $J = 6.6$  Hz), 2.84–2.88 (m, 2H), 3.84 (s, 3H), 4.80 (br s, 1H), 5.98 (s, 1H), 6.38–6.41 (m, 1H), 6.97 (d, 1H,  $J = 8.1$  Hz), 7.1 (d, 2H,  $J = 8.8$  Hz), 7.24 (s, 1H), 7.42 (d, 2H,  $J = 8.7$  Hz), 7.48 (s, 1H); LRMS (M+H) calcd for  $C_{19}H_{19}N_4O_2$  335.1, found 335.1.

**7.12.31. 8-(2,5-Dichloroisonicotinamido)-1-(4-methoxy-phenyl)-4,5-dihydro-1H-benzo[g]indazole-3-carboxamide (12: R1 = OCH<sub>3</sub>; R2 = H)**

Compound **11** (13.75 g, 0.04 mol) was added to a DMF (48 mL) solution of 2,5-dichloroisonicotinic acid, (9.47 g, 0.0411 mol), HBTU (*O*-benzotriazole-*N,N,N',N'*-tetramethyluronium-hexafluorophosphate, 18.7 g, 0.0493 mol) and diisopropylethylamine (8.52 g, 0.0493 mol) at 23 °C. The reaction mixture was stirred at 23 °C for 3 h. The completion of the reaction was monitored by thin layer chromatography. At the end of this time, the reaction mixture was concentrated to 12 ml by distillation under reduced pressure at 60 °C. The reaction mixture was cooled to 23 °C then diluted with water (1 L) and stirred for 1 h to obtain a solid precipitate. The solid residue was then stirred for 1 h with 1 L of 9:1 water and triethylamine. The solid was filtered and dried under vacuum to obtain compound **12** (19.5 g, 93.3%) as a yellow solid.  $^1H$  NMR (400 MHz, DMSO- $d_6$ ):  $\delta$  2.93 (br s, 4H), 3.81 (s, 3H), 7.08 (d, 2H,  $J = 8.3$  Hz), 7.18 (s, 1H), 7.29–7.43 (m, 5H), 7.45 (s, 1H), 7.55 (s, 1H), 7.8 (s, 1H), 8.6 (s, 1H); LRMS (M+H) calcd for  $C_{25}H_{20}Cl_2N_5O_3$  508.0, found 508.0.

**7.12.32. 8-[[5-Chloro-2-(4-methylpiperazin-1-yl)isonicotinoyl]amino]-1-(4-hydroxyphenyl)-4,5-dihydro-1H-benzo[g]indazole-3-carboxamide (16: R1 = OH; R2 = H)**

Compound **12** (1 g, 0.002 mol) was placed in a 25 mL round bottomed flask, and boron tribromide (1.85 mL, 0.02 mol) was added at 5 °C under a nitrogen atmosphere. The reaction mixture was allowed to stir at 23 °C for 16 h. Thin layer chromatography confirmed the absence of starting material. Ice (5 g) was poured into the reaction mixture with continued stirring, then diluted with dichloromethane (20 mL), filtered, and the residue obtained was repeatedly washed with dichloromethane, and was dried under vacuum. This afforded (1 g) of crude brown intermediate which was used in the subsequent reaction without purification. The crude intermediate (0.36 mmol) was mixed with *N*-methylpiperazine (0.8 mL) and refluxed for 8 h, monitoring the reaction by thin layer chromatography. At the end of the reaction, *N*-methyl piperazine was removed under reduced pressure. The slurry was triturated with water (3 × 20 mL) and filtered each time. The residue was dried under vacuum. This material was purified with silica gel column chromatography (Biotage) using ethyl acetate/methanol/ammonia (1:0.05:0.03) as eluent, affording the product **12**.  $^1H$  NMR (DMSO- $d_6$ , 400 MHz):  $\delta$  ppm 2.20 (s, 3H), 2.33–2.40 (m, 4H), 2.85–2.97 (m, 4H), 6.85–6.92 (m, 2H), 7.21–7.35 (m, 4H), 7.46 (dd,  $J = 8.2, 2.0$  Hz, 1H), 7.51 (s, 1H), 8.15 (s, 1H), 10.35 (s, 1H); HRMS (M+H) calcd for  $C_{29}H_{29}ClN_7O_3$  558.1942, found 558.2000.

**7.12.33. 1-(3-Chloro-4-methoxyphenyl)hydrazine (21)**

3-Chloro-4-methoxyaniline (20 g, 0.13 mol) was mixed with concentrated hydrochloric acid (23.4 mL) and treated at 0 °C with a solution of sodium nitrite (8.75 g, 0.13 mol) in (36.9 mL) of water. A well cooled solution of stannous chloride (85.89 g in 74.1 mL of concentrated hydrochloric acid) was added to the reaction solution and allowed to stand for 2 h. After filtration, the reaction mixture was shaken with cold caustic potash solution (164.5 mL, 25%) producing a crystalline solid. The crystalline solid was washed with water and dried in a vacuum desiccator. Recrystallization of the crude mass with (1:3 benzene/hexane) afforded **21** (6.74 g, 30.77%) as yellow crystalline solid.  $^1H$  NMR (400 MHz, DMSO- $d_6$ ):

$\delta$  3.71 (s, 3H), 3.94 (s, 2H), 6.53 (s, 1H), 6.68 (dd, 1H,  $J = 2.4, 8.8$  Hz), 6.87 (d, 1H,  $J = 2.4$  Hz), 6.92 (d, 1H,  $J = 8.8$  Hz).

**7.12.34. 1-(3-Chloro-4-hydroxyphenyl)-8-[[5-chloro-2-(4-methylpiperazin-1-yl)isonicotinoyl]amino]-4,5-dihydro-1H-benzo[g]indazole-3-carboxamide (17)**

Compound **17** was synthesized following the same synthetic protocol as described for the synthesis of compound **16**.  $^1\text{H}$  NMR (DMSO- $d_6$ , 400 MHz):  $\delta$  ppm 2.22 (3H, s), 2.38 (4H, br s), 2.83–2.99 (4H, m), 6.92 (1H, s), 7.08 (1H, d,  $J = 8.8$  Hz), 7.23–7.37 (3H, m), 7.46–7.58 (2H, m), 8.17 (1H, s), 10.40 (1H, s); LRMS (M+H) calcd for  $\text{C}_{29}\text{H}_{28}\text{Cl}_2\text{N}_7\text{O}_3$  592.0, found 592.0.

**7.12.35. 1-(4-Chloro-3-hydroxyphenyl)-8-[[5-chloro-2-(4-methylpiperazin-1-yl)isonicotinoyl]amino]-4,5-dihydro-1H-benzo[g]indazole-3-carboxamide (18)**

Compound **18** was synthesized following the same synthetic protocol as described for the synthesis of compound **16**.  $^1\text{H}$  NMR (DMSO- $d_6$ , 400 MHz):  $\delta$  ppm 2.22 (3H, s), 2.38 (4H, br s), 2.83–2.99 (4H, m), 6.92 (1H, s), 7.08 (1H, d,  $J = 8.8$  Hz), 7.23–7.37 (3H, m), 7.46–7.58 (2H, m), 8.17 (1H, s), 10.40 (1H, s); LRMS (M+H) calcd for  $\text{C}_{29}\text{H}_{28}\text{Cl}_2\text{N}_7\text{O}_3$  592.0, found 592.0.

**7.12.36. 8-[[5-Chloro-2-(4-methylpiperazin-1-yl)isonicotinoyl]amino]-1-(3-hydroxyphenyl)-4,5-dihydro-1H-benzo[g]indazole-3-carboxamide (19)**

Compound **19** was synthesized following the same synthetic protocol as described for the synthesis of compound **16**.  $^1\text{H}$  NMR (DMSO- $d_6$ , 400 MHz):  $\delta$  ppm 2.21 (3H, s), 2.38 (4H, br s), 2.85–2.98 (4H, m), 6.84–6.93 (3H, m), 7.22–7.36 (3H, m), 7.46–7.58 (2H, m), 8.16 (1H, s), 9.88 (1H, s), 10.37 (1H, s); LRMS (M+H) calcd for  $\text{C}_{29}\text{H}_{29}\text{ClN}_7\text{O}_3$  558.0, found 558.1.

**7.12.37. 8-[[5-Chloro-2-(4-methylpiperazin-1-yl)isonicotinoyl]amino]-1-(4-methoxyphenyl)-4,5-dihydro-1H-benzo[g]indazole-3-carboxamide (20)**

Compound **12** (200 mg, 0.393 mmol) was treated with *N*-methylpiperazine (0.79 mL, 7.84 mmol). The reaction mixture was heated at 80 °C for 16 h, when thin layer chromatography indicated the completion of the reaction. The reaction mixture was diluted with water (20 mL), extracted with dichloromethane (3 × 30 mL) and dried over anhydrous sodium sulfate. Evaporation of the solvent followed by silica gel column chromatography using methanol/dichloromethane (40:60) as the eluent afforded the desired product as a light yellowish solid.  $^1\text{H}$  NMR (DMSO- $d_6$ , 400 MHz):  $\delta$  ppm 2.20 (s, 3H) 2.32–2.40 (m, 1H) 2.84–2.99 (m, 4H) 3.46–3.57 (m, 4H) 3.81 (s, 3H) 6.88 (s, 1H) 7.08 (d,  $J = 8.79$  Hz, 2H) 7.18–7.25 (m, 2H) 7.32 (d,  $J = 8.05$  Hz, 1H) 7.39–7.49 (m, 3H) 8.15 (s, 1H) 10.27 (s, 1H); LRMS (M+H) calcd for  $\text{C}_{30}\text{H}_{31}\text{ClN}_7\text{O}_3$  558.1942, found 558.2.

**7.12.38. 8-[[5-Chloro-2-((3S)-3-methyl-4-[(1-methyl-1H-pyrazol-4-yl)methyl]piperazin-1-yl)isonicotinoyl]amino]-1-(4-fluorophenyl)-4,5-dihydro-1H-benzo[g]indazole-3-carboxamide (35)**

$^1\text{H}$  NMR (DMSO- $d_6$ , 400 MHz):  $\delta$  ppm 1.10 (d,  $J = 5.86$  Hz, 3H) 2.07–2.17 (m, 1H) 2.19–2.30 (m, 1H) 2.65–2.76 (m, 2H) 2.83–3.02 (m, 6H) 3.67 (d,  $J = 14.27$  Hz, 1H) 3.76 (s, 2H) 3.95 (d,  $J = 10.98$  Hz, 2H) 6.85 (s, 1H) 7.15–7.44 (m, 8H) 7.49 (br s, 1H) 7.52–7.60 (m, 2H) 8.09 (s, 1H) 10.28 (s, 1H); LRMS (M+H) calcd for  $\text{C}_{34}\text{H}_{34}\text{ClFN}_9\text{O}_2$  654.2, found 654.2.

**7.12.39. Ethyl 4-((2S)-4-[4-((3-aminocarbonyl)-1-(4-fluorophenyl)-4,5-dihydro-1H-benzo[g]indazol-8-yl)amino]carbonyl]-5-chloropyridin-2-yl)-2-methylpiperazin-1-yl methyl-1H-pyrazol-1-yl]acetate (36)**

$^1\text{H}$  NMR (DMSO- $d_6$ , 400 MHz):  $\delta$  ppm 1.04–1.27 (m, 6H) 2.05–2.19 (m, 1H) 2.21–2.31 (m, 1H) 2.52 (s, 1H) 2.72 (d,  $J = 11.89$  Hz,

2H) 2.84–3.04 (m, 5H) 3.70 (d,  $J = 14.27$  Hz, 1H) 3.96 (d,  $J = 12.08$  Hz, 2H) 4.10 (q,  $J = 7.20$  Hz, 2H) 4.99 (s, 2H) 6.87 (s, 1H) 7.18–7.27 (m, 2H) 7.27–7.44 (m, 5H) 7.49 (br s, 1H) 7.52–7.66 (m, 3H) 8.10 (s, 1H) 10.28 (s, 1H); LRMS (M+H) calcd for  $\text{C}_{37}\text{H}_{38}\text{ClFN}_9\text{O}_4$  726.3, found 726.3.

**References and notes**

- (a) Adock, I. M.; Chung, K. F.; Caramori, G.; Ito, K. *Eur. J. Pharmacol.* **2006**, *533*, 118; (b) Barnes, P. *Pharmacol. Ther.* **2006**, *109*, 238.
- (a) Baldwin, A. S., Jr. *J. Clin. Invest.* **2001**, *107*, 3; (b) Bonizzi, G.; Karin, M. *Trends Immunol.* **2004**, *25*, 280; (c) Ghosh, S.; Karin, M. *Cell* **2002**, *109*, S81.
- Swentfleben, U.; Karin, M. *Crit. Care Med.* **2002**, *30*, S18.
- (a) Castro, A. C.; Dang, L. C.; Soucy, F.; Grenier, L.; Mazdiyasi, H.; Hottelet, M., et al. *Bioorg. Med. Chem. Lett.* **2003**, *13*, 2419; (b) Karin, M.; Yamamoto, Y.; Wang, Q. M. *Nat. Rev. Drug Disc.* **2004**, *3*, 17; (c) Cosio, B. G.; Mann, B.; Ito, K.; Jazrawi, E.; Barnes, P. J.; Chung, K. F., et al. *Am. J. Respir. Crit. Care Med.* **2004**, *170*, 141.
- (a) Baxter, A.; Brough, S.; Faull, A.; Johnstone, C.; McInally, T.; PCT Int. Appl. WO 0158890 A1, 2001.; (b) Griffiths, D.; Johnstone, C., **2003**, WO 2003010163 A1 20030206.; (c) Baxter, A.; Brough, S.; Cooper, A.; Floettmann, E.; Foster, S.; Harding, C.; Kettle, J.; McInally, T.; Martin, C.; Mobbs, M.; Needham, M.; Newham, P.; Paine, S.; St-Gallay, St.; Salter, S.; Unitt, J.; Xue, T. *Bioorg. Med. Chem. Lett.* **2004**, *14*, 2817; (d) Bonafoux, D.; Bonar, S.; Christine, L.; Clare, M.; Donnelly, A.; Guzova, J.; Kishore, N.; Lennon, P.; Libby, A.; Mathialagan, S.; McGhee, W.; Rouw, S.; Sommers, C.; Tollefson, M.; Tripp, C.; Weier, R.; Wolfson, S.; Min, Y. *Bioorg. Med. Chem. Lett.* **2005**, *15*, 2870.
- (a) Kerns, J. K.; PCT Int. Appl. WO 2007076286 A2, 2007.; (b) Kerns, J. K.; Lindenmuth, M.; Lin, X.; Nie, H.; Thomas, S. M., PCT Int. Appl. WO 034317 A2, 2006.; (c) Deng, J.; Kerns, J. K.; Jin, Q.; Lin, G.; Lin, X.; Lindenmuth, M.; Neipp, C. E.; Nie, H. T.; Sonia, M.; Widdowson, K. L., PCT Int. Appl. WO 005534 A2, 2007.
- Clare, M.; Fletcher, T. R.; Hamper, B. C.; Hanson, G. A.; Heier, R. F.; Huang, H.; Lennon, P. J.; Oburn, D. S.; Reding, M. T.; Stealey, M. A.; Wolfson, S. G.; Xie, J., PCT Int. Appl. WO 037797 A1, 2005.
- (a) Morey, J. V.; Christopher, J. A. PCT Int. Appl. WO 025575 A1, 2007.; (b) Christopher, J. A.; Avitabile, B. G.; Bambrorough, P.; Champigny, A. C.; Cutler, G. J.; Dyos, S. L.; Grace, K. G.; Kerns, J. K.; Kitson, J. D.; Mellor, G. W.; Morey, J. V.; Morse, M. A.; O'Malley, C. F.; Patel, C. B.; Probst, N.; Rumsey, W.; Smith, C. A.; Wilson, M. J. *Bioorg. Med. Chem. Lett.* **2007**, *17*, 3972; (c) Waelchli, R.; Bollbuck, B.; Bruns, C.; Buhl, T.; Eder, J.; Feifel, R.; Hersperger, R.; Janser, P.; Revesz, L.; Zerves, H.-G.; Schlapbach, A. *Bioorg. Med. Chem. Lett.* **2006**, *16*, 108.
- (a) Murata, T.; Sakakibara, S.; Yoshino, T.; Ikegami, Y.; Masuda, T.; Shimada, M.; Shintani, T.; Shimazaki, M.; Lowinger, T. B.; Ziegelbauer, K. B.; Fuchikami, K.; Umeda, M.; Komura, H.; Yoshida, N. WO 03024935 A2, 2002.; (b) Murata, T.; Shimada, M.; Sakakibara, S.; Yoshino, T.; Kadono, H.; Masuda, T.; Shimazaki, M.; Shintani, T.; Fuchikami, K.; Sakai, K.; Inbe, H.; Takeshita, K.; Niki, T.; Umeda, M.; Bacon, K. B.; Ziegelbauer, K. B.; Lowinger, T. B. *Bioorg. Med. Chem. Lett.* **2003**, *13*, 913.
- (a) Bingham, A. H.; Davenport, R. J.; Fosbeary, R.; Gowers, L.; Knight, R. L.; Lowe, C.; Owena, D. A.; Parry, D. M.; Pitt, W. R. *Bioorg. Med. Chem. Lett.* **2008**, *18*, 3622; (b) Okamoto, Y.; Kubota, H.; Sato, I.; Hattori, K.; Kanayama, T.; Yokoyama, K.; Terai, Y.; Takeuchi, M. PCT Int. Appl. WO 100341 A1, 2005.; (c) Clare, M.; Hagen, T. J.; Houdek, S. C.; Lennon, P. J.; Weier, R. M.; Xu, X., PCT Int. Appl. WO 040133 A1, 2005.; (d) Bingham, A. H.; Davenport, R. J.; Fosbeary, R.; Gowers, L.; Knight, R. L.; Lowe, C.; Owen, D. A.; Parry, D. M.; Pitt, W. R. *Bioorg. Med. Chem. Lett.* **2008**, *18*, 3622.
- Castro, A. C.; Dang, L. C.; Soucy, F.; Grenier, L.; Mazdiyasi, H.; Hottelet, M.; Parent, L.; Pien, C.; Palombella, V.; Adams, J. *Bioorg. Med. Chem. Lett.* **2003**, *13*, 2419.
- Bambrorough, P.; Barker, M. D.; Campos, A. A.; Cousins, R. C.; Faulder, P.; Hobbs, H.; Holmes, D. S.; Johnston, M. J.; Liddle, J. P.; Jeremy, J.; Pritchard, J. M.; Whitworth, C., PCT Int. Appl. WO 2008034860 A1, 2008.
- Belema, M.; Bunker, A.; Nguyen, V. N.; Beaulieu, F.; Ouellet, C.; Qiu, Y.; Zhang, Y.; Martel, A.; Burke, J. R.; McIntyre, K. W.; Pattoli, M. A.; Dalouis, C.; Gillooly, K. M.; Clarke, W. J.; Brassil, P. J.; Zusi, F. C.; Vyas, D. M. *Bioorg. Med. Chem. Lett.* **2007**, *17*, 4284.
- (a) Bonafoux, D.; Bonar, S.; Clare, M.; Donnelly, A.; Guzova, J.; Kishore, N.; Lennon, P.; Libby, A.; Mathialagan, S.; McGhee, W.; Rouw, S.; Sommers, C.; Tollefson, M.; Tripp, C.; Weier, R.; Wolfson, S.; Huang, H.-C. *Bioorg. Med. Chem. Lett.* **2010**, *18*, 413; (b) Mbalaviele, G.; Sommers, C. D.; Bonar, S. L.; Mathialagan, S.; Schindler, J. F.; Guzova, J. A.; Shaffer, A. F.; Melton, M. A.; Christine, L. J.; Tripp, C. S.; Chiang, P.-C.; Thompson, D. C.; Hu, Y.; Kishore, N. *J. Pharmacol. Exp. Ther.* **2009**, *329*, 14; (c) Sommers, C. D.; Thompson, J. M.; Guzova, J. A.; Bonar, S. L.; Rader, R. K.; Mathialagan, S.; Venkatraman, N.; Holway, V. W.; Kahn, L. E.; Hu, G.; Garner, D. S.; Huang, H.-C.; Chiang, P.-C.; Schindler, J. F.; Hu, Y.; Meyer, D. M.; Kishore, N. *N. J. Pharmacol. Exp. Ther.* **2009**, *330*, 377; (d) Bergmanis, A. A.; Bonafoux, D.; Clare, M.; Crich, J. Z.; Fletcher, T. R.; Geng, L.; Hagen, T. J.; Hamper, B. C.; Hanson, G. J.; Houdek, S. C.; Huang, H.; Iula, D. M.; Koszyk, F. J.; Lennon, P. J.; Liao, S.; Liao, S.; Metz, S.; Mohler, S. B.; Nguyen, M.; Oburn, D. S.; Owen, T. J.; Partis, R. A.; Scates, A. M.; Stealey, M. A.; Tollefson, M. B.; Vazquez, M. L.; Weier, R. M.; Wolfson, S. G.; Xu, X. PCT Int. WO 200324935, 2003.
- Tayab, Z. R.; Hochhaus, G. *Expert Opin. Drug Deliv.* **2005**, *2*, 519.
- Kishore, N.; Huynh, Q. K.; Mathialagan, S.; Hall, T.; Rouw, R.; Creely, D.; Lange, C.; Carroll, J.; Reitz, B.; Donnelly, A.; Boddupalli, H.; Combs, R. G.; Kretzmer, K.; Tripp, C. S. *J. Biol. Chem.* **2002**, *277*, 13840.

17. Huynh, Q. K.; Boddupalli, H.; Rouw, S. A.; Koboldt, C. M.; Hall, T.; Sommers, C.; Hauser, S. D.; Pierce, J. L.; Combs, R. G.; Reitz, B. A.; Diaz-collier, J. A.; Weinberg, R. A.; Hodd, B. L.; Kilpatrick, B. F.; Tripp, C. S. *J. Biol. Chem.* **2000**, *275*, 25883.
18. (a) Chen, F.; Castranova, V.; Shi, X.; Demers, L. M. *Clin. Chem.* **1999**, *45*, 7; (b) Ghosh, S.; May, M. J.; Kopp, E. B. *Annu. Rev. Immunol.* **1998**, *16*, 225; (c) Karin, M. *Oncogene* **1999**, *18*, 6867.
19. Mathialagan, S.; Poda, G. I.; Kurumbail, R. G.; Selness, S. R.; Hall, T.; Reitz, B. A.; Weinberg, R. A.; Kishore, N.; Mbalaviele, G. *Protein Expr. Purif.* **2010**, *72*, 254.
20. Poda, G.; Clare, M.; Kurumbail, R. G., unpublished data.
21. Sherman, W.; Day, T.; Jacobson, M. P.; Friesner, R. A.; Farid, R. *J. Med. Chem.* **2006**, *49*, 534.